

Review

Open Access



Chemical bonding strategy on boosting superior Li⁺ diffusion kinetics towards long-stable lithium metal anode

Farwa Mushtaq^{1,2,3,#}, Haifeng Tu^{2,3,#}, Yuting Zheng^{2,3}, Yongyi Zhang^{2,3}, Zhiqiang Wang⁴, Minjie Hou⁵, Meinan Liu^{1,2,3,*}, Kunfeng Chen^{4,*}, Feng Liang^{5,*}, Jun Liu^{6,*}, Fei Liu^{7,*}, Bingsuo Zou^{1,*}, Dongfeng Xue^{8,*}

¹State Key Laboratory of Featured Metal Materials and Life-cycle Safety for Composite Structures, Guangxi Key Laboratory of Processing for Non-Ferrous Metals and Featured Materials, School of Resources, Environment and Materials, Guangxi University, Nanning 530004, Guangxi, China.

²School of Nano-Tech and Nano-Bionics, University of Science and Technology of China, Hefei 230026, Anhui, China. ³Key Laboratory of Multifunctional Nanomaterials and Smart Systems, Suzhou Institute of Nano-Tech and Nano-Bionics, Chinese Academy of Sciences, Suzhou 215123, Jiangsu, China.

⁴Institute of Novel Semiconductors, State Key Laboratory of Crystal Materials, Shandong University, Jinan 250100, Shandong, China.

⁵Faculty of Metallurgical and Energy Engineering, Kunming University of Science and Technology, Kunming 650093, Yunnan, China.

⁶Guangdong Provincial Key Laboratory of Advanced Energy Storage Materials, School of Materials Science and Engineering, South China University of Technology, Guangzhou 510641, Guangdong, China.

⁷Wuhan Institute of Marine Electric Propulsion, CSSC, Wuhan 430064, Hubei, China.

⁸Shenzhen Institute for Advanced Study, University of Electronic Science and Technology of China, Shenzhen 518110, Guangdong, China.

[#]Authors contributed equally.

***Correspondence to:** Prof. Meinan Liu, Prof. Bingsuo Zou, State Key Laboratory of Featured Metal Materials and Life-cycle Safety for Composite Structures, Guangxi Key Laboratory of Processing for Non-Ferrous Metals and Featured Materials, School of Resources, Environment and Materials, Guangxi University, 100 Daxue East Road, Nanning 530004, Guangxi, China. E-mail: meinanliu@gxu.edu.cn; Zoubs@gxu.edu.cn; Prof. Kunfeng Chen, Institute of Novel Semiconductors, State Key Laboratory of Crystal Materials, Shandong University, 27 Shanda South Road, Jinan 250100, Shandong, China. E-mail: kunfeng.chen@sdu.edu.cn; Prof. Feng Liang, Faculty of Metallurgical and Energy Engineering, Kunming University of Science and Technology, 68 Wenchang Road, Kunming 650093, Yunnan, China. E-mail: liangfeng@kust.edu.cn; Prof. Jun Liu, Guangdong Provincial Key Laboratory of Advanced Energy Storage Materials, School of Materials Science and Engineering, South China University of Technology, 381 Wushan Road, Guangzhou 510641, Guangdong, China. E-mail: msjliu@scut.edu.cn; Prof. Fei Liu, Wuhan Institute of Marine Electric Propulsion, CSSC, 20 Qixiao Road, Wuhan 430064, Hubei, China. E-mail: liuf_712@126.com; Prof. Dongfeng Xue, Shenzhen Institute for Advanced Study, University of Electronic Science and Technology of China, 1301-76 Guanguang Road, Shenzhen 518110, Guangdong, China. E-mail: dfxue@uestc.edu.cn

How to cite this article: Mushtaq, F.; Tu, H.; Zheng, Y.; Zhang, Y.; Wang, Z.; Hou, M.; Liu, M.; Chen, K.; Liang, F.; Liu, J.; Liu, F.; Zou, B.; Xue, D. Chemical bonding strategy on boosting superior Li⁺ diffusion kinetics towards long-stable lithium metal anode. *Chem. Synth.* **2025**, *5*, 27. <https://dx.doi.org/10.20517/cs.2024.66>

Received: 26 May 2024 **First Decision:** 31 Jul 2024 **Revised:** 27 Aug 2024 **Accepted:** 14 Sep 2024 **Published:** 20 Feb 2025

Academic Editors: Huiqiao Li, Weihua Chen **Copy Editor:** Pei-Yun Wang **Production Editor:** Pei-Yun Wang



© The Author(s) 2025. **Open Access** This article is licensed under a Creative Commons Attribution 4.0 International License (<https://creativecommons.org/licenses/by/4.0/>), which permits unrestricted use, sharing, adaptation, distribution and reproduction in any medium or format, for any purpose, even commercially, as long as you give appropriate credit to the original author(s) and the source, provide a link to the Creative Commons license, and indicate if changes were made.



Abstract

With the fast development of electronics, electric vehicles and electric airplanes, lithium metal batteries (LMBs) with a high energy density attract increased attention for their long-voyage-capability. However, the dendrites from uneven Li plating may cause serious safety issues, especially under low-temperature conditions, thus limiting the practical application of LMB. Tremendous efforts to develop various Li hosts based on thermodynamics, trying to provide lithophilic sites for homogeneous deposition, did not yet push the cycle life of Li anodes long enough to compete with current graphene anodes, especially under harsh conditions, such as subzero temperatures. The focus of this review is on the recent progress in chemical bonding strategies for boosting lithium ions/atoms (Li^+/Li) transport via liquid, interphase, and solid phases through rational design of electrolytes, interphases, and Li hosts. Research results on understanding the working mechanism of chemical interaction between Li^+/Li and other molecules in bulk electrolytes, interphases, or electrodes during charge/discharge are discussed. These understandings may provide new perspectives on designing advanced LMB systems.

Keywords: Li^+/Li transport kinetics, diffusion kinetics, solvation structure, desolvation, nucleation kinetics, deposition kinetics

INTRODUCTION

Lithium-ion battery (LIB) technology has revolutionized people's daily life since 1990; however, the development of new battery systems with a higher energy density is imperative for coping with the insatiable requirements from current wearable electronics and electric vehicles^[1]. Compared to a graphite anode with a theoretical-specific-capacity of $372 \text{ mAh}\cdot\text{g}^{-1}$ used in a typical LIB system, a lithium metal anode (LMA) shows its superiority, i.e., a superhigh theoretical-specific-capacity of $3,860 \text{ mAh}\cdot\text{g}^{-1}$ and a low reduction potential (-3.04 V vs. standard hydrogen electrode). When paired with a high-voltage LiCoO_2 (LCO) cathode, a lithium metal battery (LMB) can deliver two times higher energy density ($400\text{--}500 \text{ Wh}\cdot\text{kg}^{-1}$) of LIB^[1]. Although the LMB system shows promising future applications, it still faces many challenges. On one hand, the continuous side reactions between the Li anode and electrolytes, due to its high reactivity, shorten the battery's lifespan; on the other hand, the unbalanced Li^+ diffusion and deposition kinetics leads to lithium dendrites, which poses serious safety concerns. Besides, the requirements on fast-charging and low-temperature applications cause more severe dendrite issues in LMBs^[2,3]. Because at low temperatures, the Li^+ transport is low. Therefore, addressing these dendrites and impeding side reactions seem to be very important and urgent.

In the early research, Chazalviel proposed a characteristic time τ to describe the growth of lithium dendrite. The characteristic time τ is also known as Sand's time. Chazalviel's theory states that the dendrite nucleation begins when the concentration of Li^+ at the surface of the LMA reaches zero leading to uneven distribution of potential^[4]. The equation can be found below:

$$\tau = \pi D \left(\frac{C_0 e}{2J} \right)^2 \left(\frac{\mu_a + \mu_{\text{Li}}^+}{\mu_a} \right)^2 \quad (1)$$

where τ is the initial time of dendrite growth, D is the ambipolar diffusion coefficient, e is the electronic charge, C_0 is the initial ionic concentration, J is the effective current density, and μ_a and μ_{Li}^+ are the mobility of anion and Li^+ , respectively.

Based on this equation, targeted increase on C_0 , μ_{Li}^+ and decrease on μ_a , J can prolong the dendrite nucleation time τ , thus effectively suppressing dendrite formation. To increase C_0 , the simplest way is to use a high-concentrated salt electrolyte system. Indeed, this specific system could stabilize Li anodes as evidenced by numerous reported works; however, the high cost of lithium salt limits the broad application of this high-concentrated salt system^[5]. Regulating the mobility of anions and lithium ions and reducing the current density on the Li anode appear to be more feasible in LMBs. In addition, several differential equations and models are used to describe the dynamics of Li^+ transport^[6], battery degradation behavior^[7], and thermal behaviors (such as heat generation rates and temperature variations)^[8]. Besides understanding the theory of transport kinetics, there is a need to understand different steps involved in charge transport during charge and discharge.

Understanding Li^+ diffusion path during charging/discharging may well help us manipulate the mobility of anions and lithium ions. As shown in Figure 1, there are eight steps for Li^+ diffusion from a cathode to a Li anode (charging process): (1) Li^+ extracted from cathode crystal lattice; (2) Li^+ diffusion through cathode-electrolyte interface (CEI); (3) Li^+ coordinating with solvent molecules in bulk electrolyte to form solvated Li^+ ; (4) solvated Li^+ transport in bulk electrolyte (passing through separator); (5) solvated Li^+ taking desolvation to release naked Li^+ at the interphase; (6) Li^+ transport across solid electrolyte interphase (SEI); (7) Li^+ taking a reduction reaction to form Li atom ($Li^+ + e^- = Li$); and (8) Li atom migrating along Li anode surface to finish Li plating^[9,10]. During discharge (Li stripping) process, these steps are reversed and Li^+ migrates from an anode to a cathode and encounters the same pathway in reverse. From these steps, effectively improving Li^+ transport kinetics in steps 4-8 can well address dendrite issues and Li deposition behavior. Besides dendrite, Li^+ transport kinetics closely relate to the popular function of fast charging/discharging and the application in low temperatures. Therefore, manipulating Li^+ transport kinetics is very important for practical applications.

To enhance Li^+ transport kinetics, a chemical bonding approach has been proposed to modify Li^+ environment for providing its new transport paths, thus fastening Li^+ mobility, hence effectively suppressing dendrite growth. For example, researchers reported a series of inorganic additives, such as lithium montmorillonite, $Li_{1.3}Al_{0.3}Ti_{1.7}(PO_4)_3$ (LATP), BN, LiF, forming interaction with solvent molecules to regulate the coordination environment of Li^+ in an electrolyte system, and thus create unique Li^+ transport channels through these anion-participated Li^+ solvation clusters for accelerating Li^+ diffusion kinetics^[5,11,12]. Here, we present recent advances in research on chemical bonding strategy for boosting lithium ions/atoms (Li^+/Li) transport via liquid, interphase and solid phases through rational design of electrolytes, interphases and Li hosts. We discuss the chemical bonding strategy in the following four parts corresponding to steps 4-7: (a) diffusion of Li^+ ions in the bulk electrolyte; (b) desolvation of Li^+ ions at the interface of an anode; (c) migration of Li^+ ions through SEI; and (d) diffusion of Li^+ ions in the LMA; and finally give a conclusion and perspective.

STRATEGIES TO OVERCOME SLUGGISH Li^+/Li TRANSPORT KINETICS

Tuning the Li^+ solvation environment in electrolyte can enhance the Li^+ diffusion rate, interfacial desolvation, and SEI conductivity. Nevertheless, determining the ideal electrolyte formula to reduce dendrite growth and quantifying such kinetic properties of the Li^+ in various electrolytes are both highly challenging. Besides Li^+ transport kinetics, lithium deposition kinetics at anodes is also an important topic^[13]. Practices of increasing Li^+/Li transport/diffusion within the bulk electrolyte, electrolyte/electrode interface, and electrode (anode) are summarized and reviewed in this section in the following ways: strategies for electrolyte bulk design; interfacial desolvation strategies; tailoring the electrolyte solvation towards conductive and stronger SEI and kinetic modulation of hosts/current collectors.

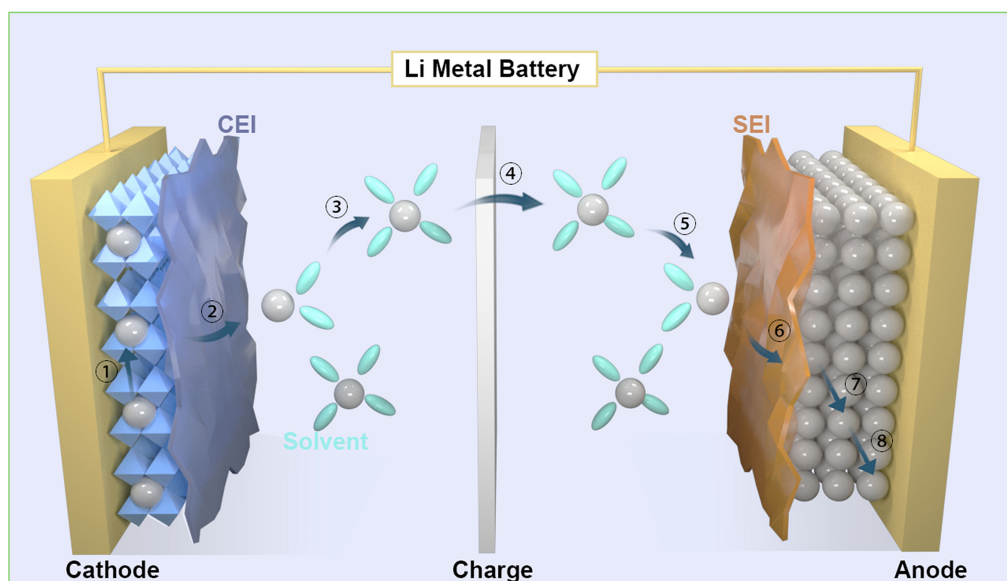


Figure 1. Schematic diagram of the transport steps from cathode to anode that Li^+ ions undergo during charging.

Electrolyte, called “blood” of a battery, plays a crucial role in ion migration and charge transfer during battery working process^[14]. As shown in [Figure 2A](#), the electrolyte consists of three primary components: lithium salt anions, solvent molecules, and additives. These three components work together in harmony, akin to three “horses” pulling a Li^+ carriage^[15]. Lithium salts are firstly dissociated by solvents to obtain free ions, including Li^+ and anions, while these dissociated Li^+ need to coordinate with solvent molecules/anions to form solvated Li^+ . Since this solvation structure has a great influence on the interphase components and the desolvation energy, rational design on electrolyte is quite important and necessary^[16].

The solvent constitutes the major component of the electrolyte, accounting for approximately 85% of the total mass. Tailoring the electrolyte solvent composition or designing solvent molecules is an effective approach to achieving rapid Li^+ ion conduction in the electrolyte bulk phase. For example, solvents with high dielectric constants (ϵ) and low viscosities (η) can promote the dissociation of lithium salts, leading to high ionic conductivity. However, the high ϵ also implies a strong affinity between Li^+ ions and solvent molecules, which limits the desolvation kinetics of Li^+ ions and increases the impedance to Li^+ mass transfer from the bulk electrolyte to the electrode^[17]. From the perspective of electrolyte solvation chemistry, the formation of the solvation sheath around Li^+ ions arises from a competition between solvent molecules and anions from lithium salts. It is interesting that the concentration effect of lithium salts can also cause a change in the solvation structure of Li^+ ions, further affecting the transport of Li^+ ions^[18–21]. Sun *et al.* used two salts to construct a multilayer solvation structure electrolyte and achieved a high Li^+ ion transference number of 0.9 in a 1 M low-concentration electrolyte (LCE) [[Figure 2B](#)]^[22]. By decreasing the solvent’s inherent solvation capacity, more anions can coordinate with lithium ions. This solvation structure not only allows for the formation of a SEI derived from anions but also promotes the rapid desolvation of Li^+ ions, resulting in efficient transport of Li^+ ions within the bulk electrolyte and the SEI layer [[Figure 2C](#)]^[23]. By deeply exploring and categorizing the interactions among Li^+ -solvent, Li^+ -anion, and solvent-solvent in the electrolyte, it is possible to gain an atomic-level understanding of the solvation effect, which can serve as guidelines for the design of advanced electrolytes. Besides, multifunctional additives can also be employed to weaken the interaction between Li^+ ions and solvent molecules, facilitating the desolvation progress of Li^+ ions [[Figure 2D](#)].

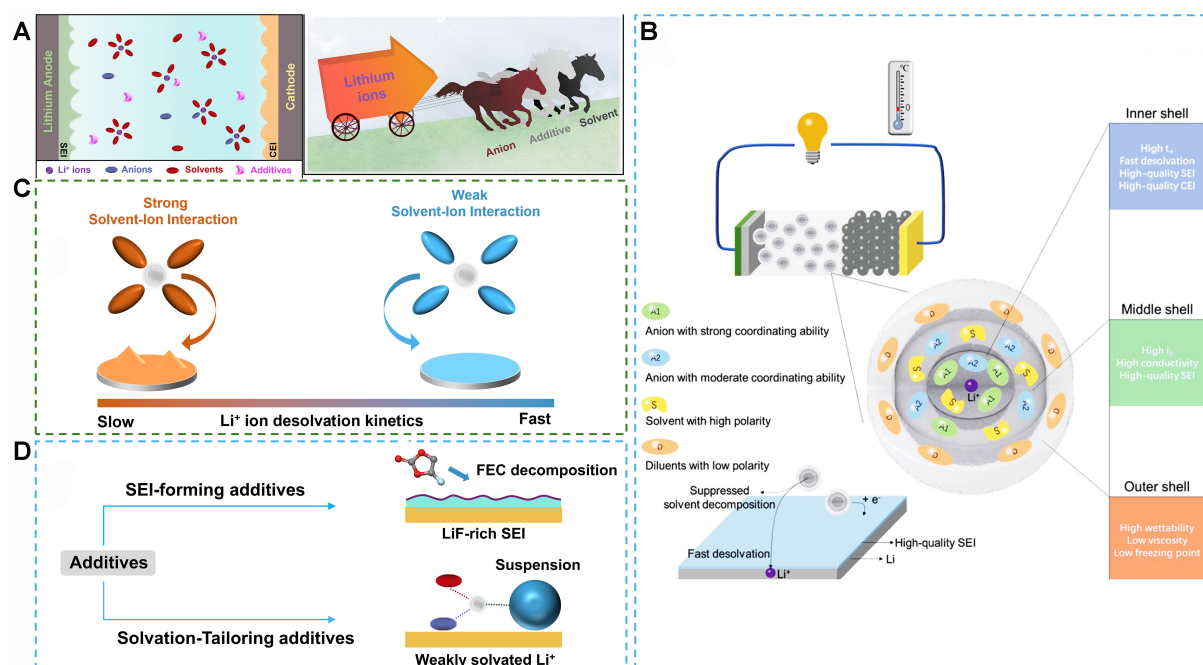


Figure 2. (A) The Schematic diagram of electrolyte composition of LMBs; (B) Schematic diagram of constructing multilayer solvation structure. Reproduced with permission^[22]. Copyright 2022, WILEY-VCH; (C) The Li⁺ ions desolvation progress in strongly and weakly solvating power solvent; (D) Schematically depicting the effect of SEI-forming additives and solvation-tailoring additives. LMBs: Lithium metal batteries; SEI: solid electrolyte interphase.

Regulation of Li⁺ transport kinetics in bulk electrolyte

Designing additives to form chemical bonding with “solvent” for fast Li⁺ diffusion

Generally, Li⁺ coordinates with solvent molecules and anions in three different modes [Figure 3A]: solvent-separated ion pairs (SSIPs) by coordinating with solvent molecules, contact ion pairs (CIPs) by coordinating with one anion, and aggregates (AGGs) by coordinating with multiple Li⁺ ions and anions^[24]. LCEs consist mainly of SSIPs and free solvent molecules, known as a salt-in-solvent system. As the concentration of lithium salt increases, the quantity of solvent molecules decreases, and anions gradually penetrate the Li⁺ ions solvation shell, resulting in a significant decrease of SSIPs, while the number of CIPs and AGGs increases, which is referred to as a solvent-in-salt electrolyte. Li⁺ ions diffuse in electrolytes in two modes: vehicular motion and structural motion [Figure 3B]. Vehicular motion refers to the diffusion of Li⁺ ions along with their tightly bound solvation shell as one entity (making it difficult to move), which is usually considered as the main ionic diffusion mechanism in dilute liquid electrolytes. In contrast, structural motion involves the diffusion of Li⁺ through successive ion dissociation/association exchange across different shells (where Li⁺ mobility is higher)^[25]. As shown in Figure 3C, the movement of Li⁺ ions can be metaphorically illustrated using these two diffusion mechanisms in battery systems: Vehicular motion resembles a 400-meter race; structural motion is akin to a 4 × 100-meter relay race. In vehicular mode, one person moves from back to front, while in structural mode, several people move from back to front. Apparently, the structural mode is more efficient for Li⁺ diffusion.

Li⁺ with CIPs and AGGs diffuses along via the structural motion. This mechanism explains why high-concentrated electrolyte (HCE) systems always present a high Li⁺ transference number. As shown in Figure 4A, the electrolyte system composed of 7 M Li[CF₃SO₂]₂N (LiTFSI) in 1,2-dimethoxyethane (DME)/1,3-dioxolane (DOL) exhibits an unexpectedly high t_+ of 0.73. This is attributed to reduced solvation sheath around Li⁺ in HCE, which makes Li⁺ more mobile^[19]. This HCE concept can also be applied in solid-state

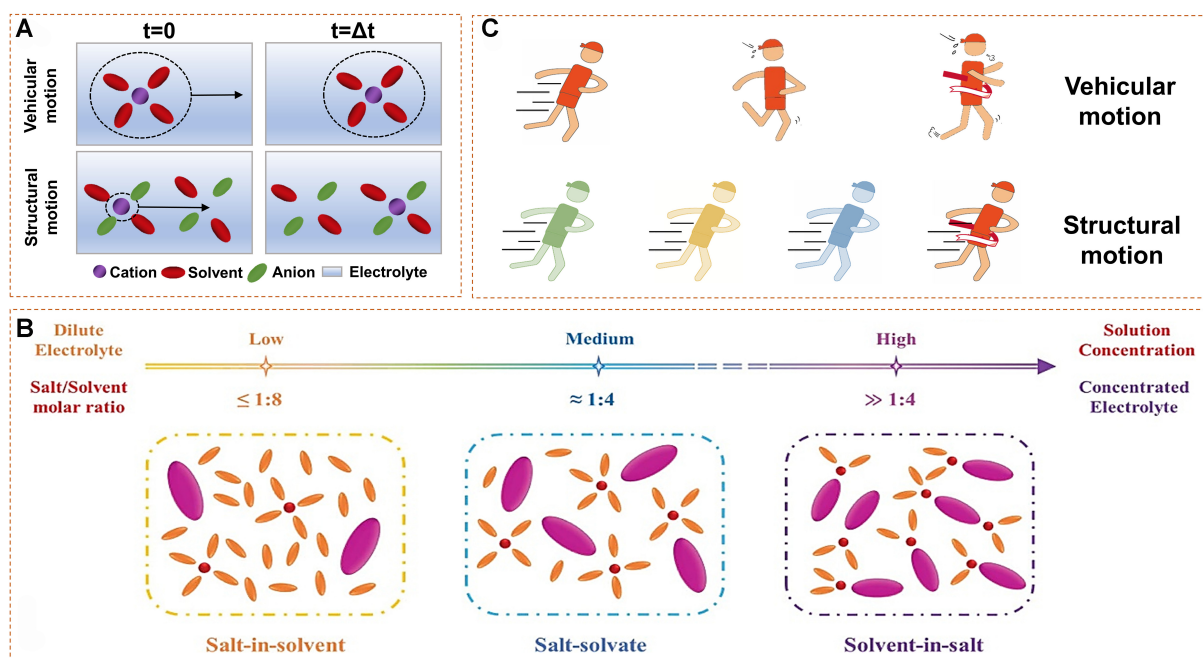


Figure 3. (A) Schematic of two kinds of Li^+ diffusion mechanism from different solvation structures: vehicular and structural motion from $t = 0$ to $t = \Delta t$; (B) The change of Li^+ solvation structure with salt concentration. Reproduced with permission^[24]. Copyright 2023, IOP Science; (C) A metaphor illustration on these two diffusion mechanisms in battery system: 400 meters race represents vehicular motion; 4×100 meters relay race represents structural motion.

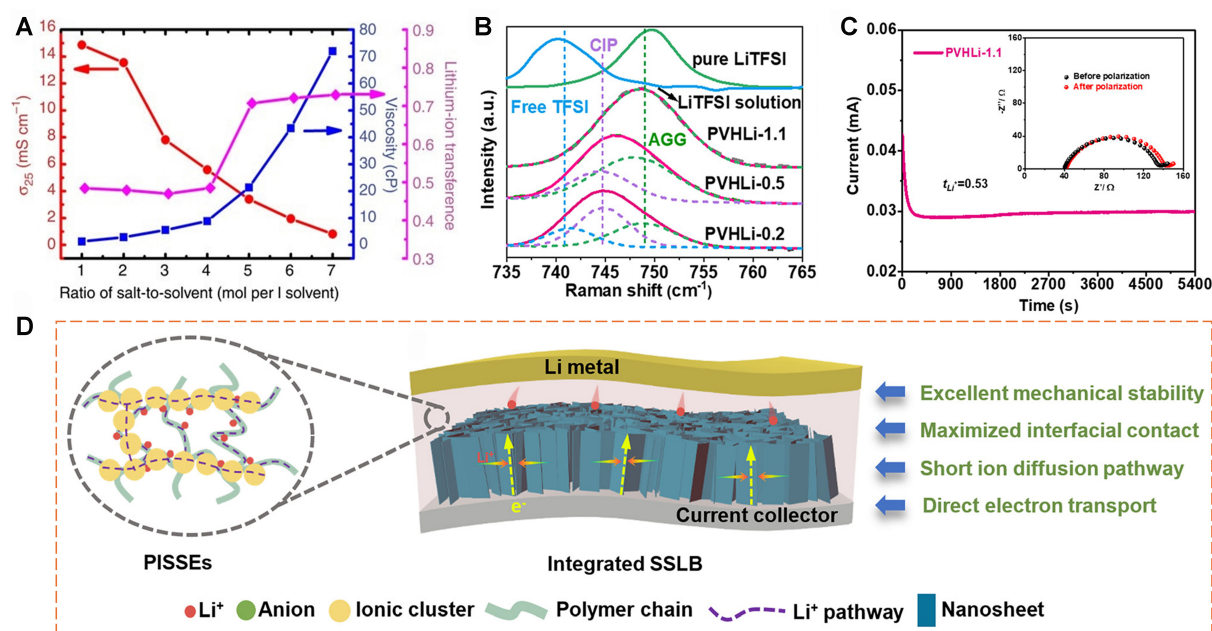


Figure 4. (A) Viscosity, ionic conductivity and t_+ of electrolytes with different ratios. Reproduced with permission^[19]. Copyright 2013, Springer Nature; (B) Raman characterization of solvation structure of PVHLi-x. Reproduced with permission^[26]. Copyright 2021, WILEY-VCH; (C) The measurement of t_+ of PVHLi-1.1. Reproduced with permission^[26]. Copyright 2021, WILEY-VCH; (D) The schematic diagram of Li^+ ion transport pathways in PISSEs. Reproduced with permission^[26]. Copyright 2021, WILEY-VCH. PISSEs: Polymer-in-salt electrolytes.

lithium batteries (SSLBs). Liu *et al.* reported a poly (vinylidene fluoride-co-hexafluoro-propylene) (PVDF-

HFP)-based polymer-in-salt electrolyte (PISSE)^[26]. With the increase of lithium salt concentration, PVHLi-1.1 (PVHLi-*x*, where *x* is the mass ratio of polymer to lithium salt) contains a large number of AGG structures, indicating the strengthened binding of Li⁺/anion at high salt concentration [Figure 4B]. Besides the transport path along polymer chains such as conventional solid polymer electrolytes (SPEs), PISSEs offer another transport channel due to these AGGs, enabling Li⁺ rapid migration, as evidenced by the high *t*₊ of 0.53 [Figure 4C and D].

Apart from this high-concentrated approach for constructing CIP and AGG, researchers found that regulating the solvation structure of Li⁺ ions through the rational utilization of intermolecular interactions can also achieve AGG mode [Figure 5A]. Specifically, the LATP nanoparticles are embedded in a PVDF-HFP matrix with one-dimensional channel structure, and the interactions between these LATP particles and succinonitrile (SN) inside the channel affect the solvation structure of Li⁺ ions in the electrolyte, promoting the formation of AGG structures, which significantly enhance the transport rate of Li⁺ ions^[27]. With this concept, Li⁺ solvation structure can be easily tuned by designing chemical bonds between inorganic additives and “polymer solvent” rather than increasing the concentration of lithium salts. In recently reported BN-assisted polymer electrolyte^[11], BN not only affects the interaction between Li⁺ and -CF groups, allowing Li⁺ to readily hop along polymer segments, but it also shifts the Li⁺ solvation structure from polymer units to AGG ion pairs, accelerating Li⁺ diffusion [Figure 5B]. As shown in Figure 5C, lithium montmorillonite in a polymer matrix can also change Li⁺ solvation structure through solvent molecules to anion participated clusters, as evidenced by Raman spectra. These as-constructed AGGs transport channels efficiently make rapid Li⁺ ions transfer kinetics. Quasi-solid electrolytes can also affect the ion transport behavior and deposition pattern^[28]. Researchers reported that, in a quasi-solid electrolyte (SiO₂-SO₃Li/PVDF-HFP), the component interactions among the polymer network, liquid electrolyte, and sulfonated SiO₂ nanoparticles were helpful for enhanced Li⁺ conductivity and excellent liquid electrolyte retention without volatilization^[29]. An infiltrating structure of a quasi-solid electrolyte comprising a concentrated electrolyte in a poly(tri-acrylate) network resulted in an ion transfer number of 0.79^[30].

Except polymer electrolytes, this inorganic additive strategy can also be applied in liquid electrolyte systems to boost the Li⁺ diffusion kinetics. Recently, researchers reported the successful development of a weakly solvating environment using nano-suspended additives such as Li₂O, Li₃N, and LiF which accelerated the migration of Li⁺ ions in the electrolyte^[31–33]. They first reported a suspended electrolyte composed of Li₂O nanoparticles, which altered the solvation environment of Li⁺ and produced a LiF-rich SEI^[31]. In traditional electrolytes [1 M LiPF₆ in ethylene carbonate (EC)/diethyl carbonate (DEC) with 10% fluoroethylene carbonate (FEC)], strong solvation interactions between Li⁺ ions and solvent molecules form SSIPs, making desolvation difficult. Furthermore, decomposition of solvent species results in organic-rich SEI. Li₂O suspended electrolyte can modify the Li⁺ solvation environment through its strong surface adsorption, causing Li⁺ ions to become weakly solvated by solvents and thus creating a weak solvation environment. In addition to Li₂O nanoparticles, the suspended electrolytes containing Li₃N have also been systematically studied due to their outstanding thermodynamic stability, high Li⁺ conductivity, and ability to suppress lithium dendrite growth in previous reports. Li₃N is lithiophilic, which can guide Li⁺ ions to deposit around Li₃N particles and avoid dendrite growth. Additionally, similar to the action of Li₂O, Li₃N can also create a weakly solvated environment by reducing the interaction between Li⁺ ions and solvents in the electrolyte, which accelerates Li⁺ ion transport [Figure 6A]^[32]. The Raman spectrum also indicates that in the Li₃N suspended electrolyte, the interactions between Li⁺ ions and the oxygen atoms in the C=O and C-O groups of EC are both reduced, suggesting that Li₃N weakens the coordination between Li⁺ ions and the solvent [Figure 6B]. Nano LiF particles have also been utilized recently as a model to capture free solvent molecules and build a low-activity solvent system [Figure 6C and D]^[33].

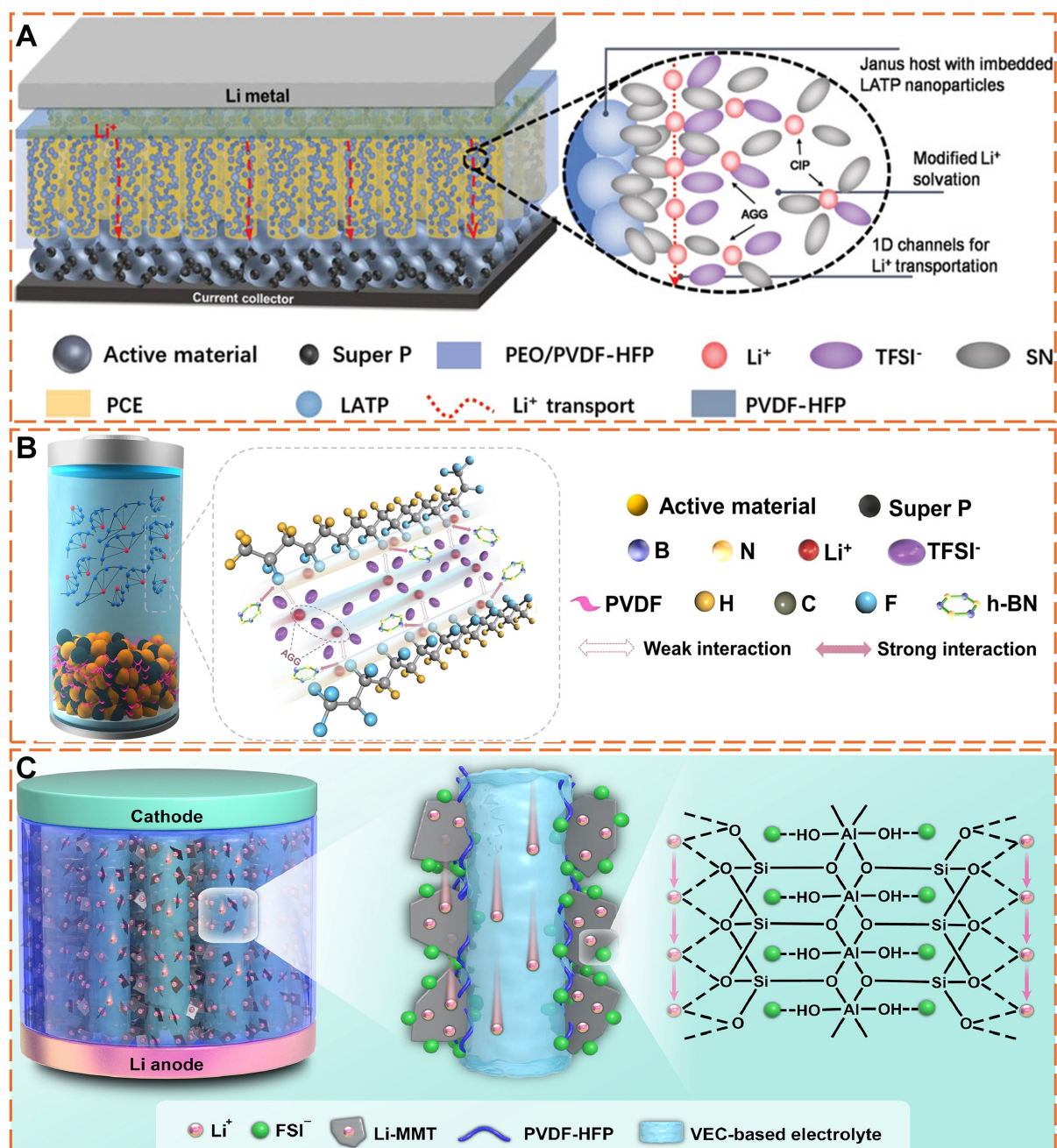


Figure 5. (A) Schematic illustration of the as-designed JSE structure. Reproduced with permission^[27]. Copyright 2022, WILEY-VCH; (B) Schematic representation of the Li^+ transport channel of the PHLBH electrolyte. Reproduced with permission^[11]. Copyright 2023, Elsevier; (C) Schematic representation of dual Li^+ transport pathways in the Li-MPSE. Reproduced with permission^[12]. Copyright 2023, Elsevier. JSE: Janus quasi-solid electrolyte; PHLBH: PVDF-HFP/LiTFSI/BN; MPSE: montmorillonite/PVDF-HFP solid electrolyte.

Rational design of solvent for weakening the interaction between Li^+ and its solvation shell

Ion transport is highly dependent on the solvation structure, which can be optimized by regulating the complex interactions between Li^+ and the solvent. To enhance the kinetics of Li^+ ion transport, one approach is to select appropriate solvent components, while another approach is to reduce the solvation energy of Li^+ through rational design of solvent molecules. Huang *et al.* designed a hybrid solvent electrolyte 7FEC/3AN [1 M LiPF_6 in FEC/acetonitrile (AN), 7/3 by vol.]^[34]. The FEC-dominant solvation shell can form

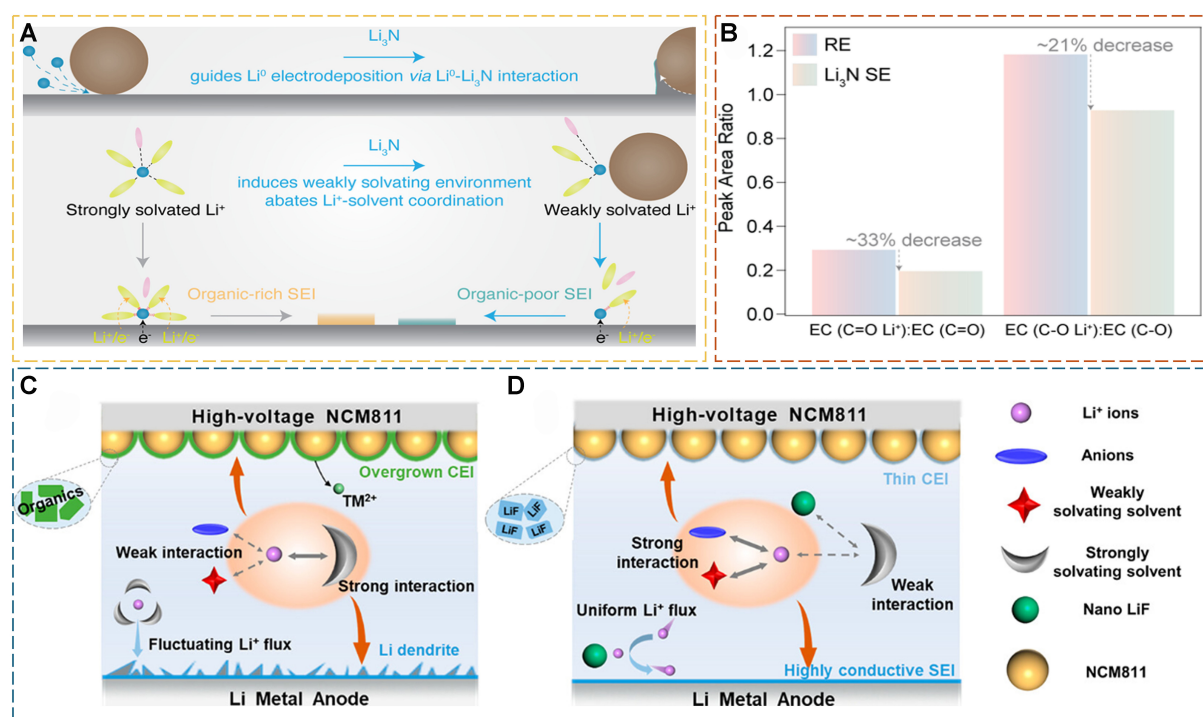


Figure 6. (A) The schematic illustration of Li_3N suspension electrolyte impacting the solvation structure and SEI composition. Reproduced with permission^[32]. Copyright 2023, American Chemical Society; (B) Raman peak area ratios of RE and Li_3N SE. Reproduced with permission^[32]. Copyright 2023, American Chemical Society; Schematic representation of the Li^+ solvation environment and electrode interface chemistry in (C) control and (D) LiF -based suspension electrolyte. Reproduced with permission^[33]. Copyright 2024, American Chemical Society. SEI: Solid electrolyte interphase; RE: reference electrolyte; SE: suspension electrolyte.

a stable SEI, and the AN constructs the ion hopping channel for fast Li^+ migration. The solvation frequency was also proposed as the efficiency of Li^+ ions hopping between solvents. The 4.4 V graphite (Gr)/NMC811 cell keeps a capacity retention of 70% after 1,000 cycles at 15 C [Figure 7A]. As illustrated in Figure 7B, achieving fast Li^+ ion transport in batteries depends on high Li^+ conductivity, low desolvation energy, and low energy barrier of Li^+ ions crossing the SEI^[35]. A 1.8 M lithium bis(fluorosulfonyl)imide (LiFSI)-DOL electrolyte was also proposed, which facilitated Li^+ ion transport and the Li/Gr cell delivered a remarkable capacity of $320 \text{ mAh}\cdot\text{g}^{-1}$ at 4 C rate. In comparison, the conventional 1.0 M LiPF_6 EC/dimethyl carbonate (DMC) electrolyte exhibited a much lower capacity of only $20 \text{ mAh}\cdot\text{g}^{-1}$.

Recent studies have focused on rational design of solvent molecules at the molecular level to reduce the solvation energy of Li^+ ions and solvent molecules. This approach can be divided into two types based on whether a solvent is fluorinated. As shown in Figure 7C, the solvent solvation ability can be adjusted through the steric hindrance effect of solvent molecules. For example, Chen *et al.* designed a new solvent 1,2-diethoxyethane (DEE) by replacing the methoxy groups on the DME molecule with larger ethoxy groups^[36]. The increased steric hindrance of DEE resulted in lower solvation ability of Li^+ ions compared to DME. Similarly, Park *et al.* introduced a methyl group into the middle segment of the DME molecule to design a low dielectric constant solvent 1,2-dimethoxypropane (DMP), which accelerates the kinetics of Li^+ ion transport by reducing its solvation energy through increased steric hindrance effect^[37]. These bulky functional groups of solvents occupy space, thereby restricting the movement or reactions of other molecules or groups, which, in turn, reduces the solvation energy and accelerates Li-ion transport kinetics. In addition, the stability of the coordination structure between Li^+ ions and solvent molecules is also one of the criteria for evaluating the solvent solvation ability. Ma *et al.* calculated the solvation ability of

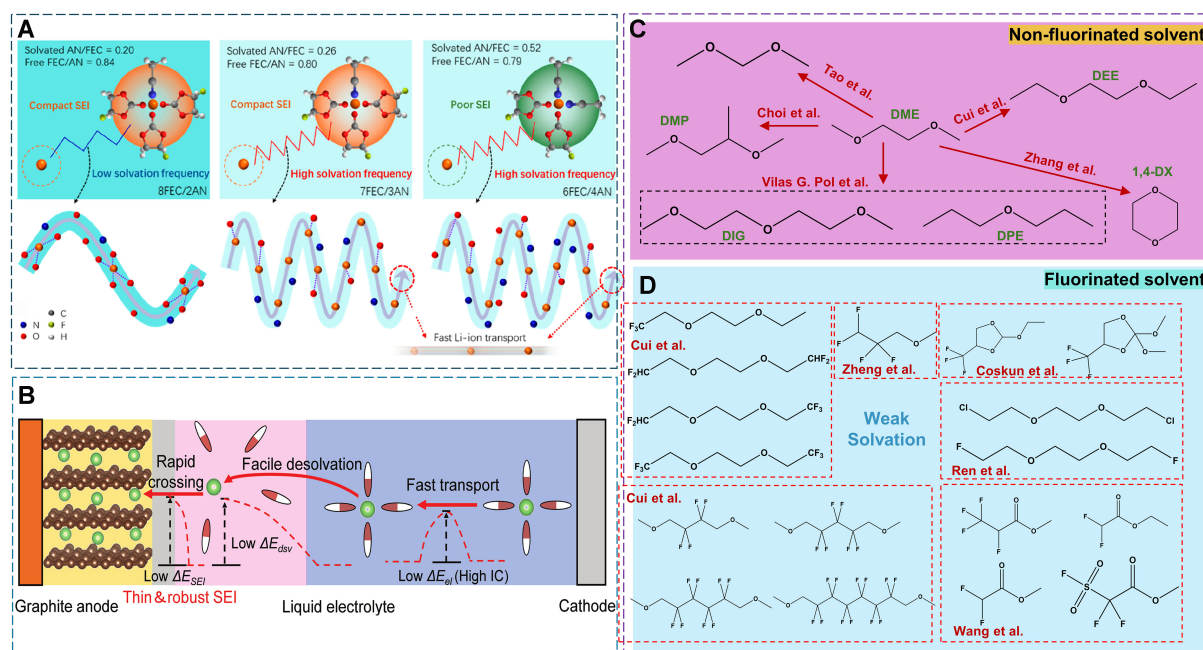


Figure 7. (A) The schematic illustration of the solvation structure in different ratios of FEC/AN. Reproduced with permission^[34]. Copyright 2022, American Chemical Society; (B) All steps that affect kinetics of Li^+ ions from cathode to anode during charging. Reproduced with permission^[35]. Copyright 2022, WILEY-VCH; (C) The summary of non-fluorinated weakly coordinating solvents. Reproduced with permission^[23,36-39]; (D) The summary of fluorinated weakly coordinating solvents. Reproduced with permission^[16,40-45]. FEC: Fluoroethylene carbonate; AN: acetonitrile.

dimethoxymethane (DMM) and DME using density functional theory (DFT) calculations, and the DMM had weaker solvation ability for Li^+ ions due to the poorer stability of the Li^+ -DMM four-membered compared to the Li^+ -DME five-membered structure^[23]. Compared to linear ethers, cyclic ethers have smaller dielectric constants. Yao *et al.* reported the non-polar solvent 1,4-dioxane (1,4-DX) as a weakly solvating electrolyte to accelerate the desolvation of Li^+ ions and achieve fast charging in batteries^[38]. Li *et al.* found that the monodentate ether DPE had a weaker chelation ability than the tridentate ether DIG. Using highly non-polar DPE as a solvent, low-concentration (1.8 M LiFSI) ether-based electrolytes can be used in 4.3 V high-voltage LMBs^[39]. The high electronegativity of fluorine (F) can weaken the electron cloud density of oxygen atoms in ether compounds, resulting in their weak solvation ability. Based on the fundamental structure of DEE molecules, Yu *et al.* designed a series of fluorinated-DEE molecules by introducing $-\text{CF}_3$ or $-\text{CHF}_2$ groups at the β -position of DEE [Figure 7D], and found that CHF_2 groups exhibit superior electrical conductivity and performance compared to the fully fluorinated $-\text{CF}_3$ group^[40]. The weakly solvating solvent can promote the formation of anion-derived SEI, but solvents that are excessively weak can hinder ion dissociation and conduction. Thus, it is important to find a balance between electrode stability and ion transport. Based on the molecular structure of fluorinated 1,4-dimethoxybutane (FDMB), Wang *et al.* also increased the number of $-\text{CF}_2$ units in backbones to enhance the oxidative stability of the solvent molecules. The designed fluorinated 1,6-dimethoxyhexane (FDMH) was used as the main solvent, with DME as the co-solvent^[41]. By reasonable optimization of the electrolyte formulation, the anode-free Cu/NCM811 pouch cell keeps a 75% capacity retention after 120 cycles. It has been reported that 1,2-bis(2-fluoroethoxy) ethane (FDDE) solvent exhibits better salt solubility and oxidation resistance than 1,2-bis(2-chloroethoxy)-ethyl ether (ClDEE) solvent^[42,43]. To address the low conductivity of Li^+ ions in fluorinated solvents, Shi *et al.* designed an amphiphilic fluorinated ether molecule [1,1,2,2-tetrafluoro-3-methoxypropane (TFMP)]. The highly fluorinated segment ensures the oxidative stability of the electrolyte ($-\text{CF}_2\text{CHF}_2$), while the other segment ($-\text{CH}_2\text{OCH}_3$) retains a methoxy group to enable weak coordination with Li^+ ions^[44]. The TFMP

solvents can form a core-shell-like solvation structure with Li^+ ions in the electrolyte. The design strategy of combining the high oxidative stability of fluorinated ethers with the high solvation ability of ether solvents for Li^+ ions has also been reported by Zhao *et al.*, such as 2,2-dimethoxy-4-(trifluoromethyl)-1,3-dioxolane (DTD_L) and 2-ethoxy-4-(trifluoromethyl)-1,3-dioxolane (cFTOF)^[45]. Recently, Xu *et al.* developed a series of fluorinated ester solvents as electrolytes for Li-ion batteries under extreme operating conditions by balancing the donor number (DN) value, dielectric constants (ϵ), and Li^+ -solvent binding energies^[16]. The methyl difluoroacetate (MDFA) was chosen as the soft solvent, methyl 2,2-difluoro-2 (fluorosulfonyl)acetate (MDFSA) as the co-solvent, and 1,1,2,2-tetrafluoroethyl-2,2,3,3-tetrafluoropropylether (TTE) as the anti-solvent. Additionally, 1 M LiTFSI in MDFA/MDFSA-TTE was used in the Gr/NCM811 battery and achieved a capacity retention of 93.9% at -30 °C after 260 cycles. The molecular design of weakly solvating electrolytes has received widespread attention and rapid development, as it fundamentally reduces the energy barrier of desolvation and enables fast Li^+ transport kinetics.

Interfacial desolvation strategies

Solvated Li^+ travels to the electrode surface after diffusing through the bulk electrolyte region. Prior to deposition, Li^+ must overcome a significant energy barrier to disintegrate Li^+ solvation sheath^[46]. During charging, Li^+ desolvates from the coordination shell and gets adsorbed on the SEI surface (the adsorbed ions are called adatoms). Following that, the adatoms travel through SEI to Li anode surface and experience electron transfer reaction, and finally, Li^+ is reduced and plated/deposited on the Li surface. During the discharge phase, the same reactions take place in reverse. Earlier studies using the conventional ac impedance method disclosed that the desolvation process has the major contribution (as a dominant factor and as a rate-determining step, it occupies a significant share of energy consumption) to slow down the interfacial charge transfer kinetics (interfacial resistance), resulting in the large activation overpotential. Thus, this desolvation process affects the charge transfer at interphase and worsens ion polarization^[5,47,48]. At low temperatures, the Li^+ desolvation dominance in Li^+ transfer kinetics can be worse^[9]. As a result, it is one of the most effective parameters for influencing the kinetics of electrochemical reactions.

Design of sieving layer with functional groups for desolvation

Introduction of a sieving layer seems a feasible way to actively peel off the solvation shell. Thankfully, the emergence of porous materials, such as covalent organic frameworks (COFs) and metal-organic frameworks (MOFs), offers new possibilities for formulating ion sieves not only by separator modification but also by direct electrolyte modifications and as Li^+ transporting porous layers/coatings on an electrode [Figure 8A]. Their pore structure acts as a sieve to filter out extraneous solvent molecules inside the Li^+ solvation layer. Because of their tunable chemical characteristics, long-lasting electrochemical/thermal stability, abundant cavity construction/porosity, open metal sites or functional groups, and vast surface area, COFs/MOFs have steadily been employed in LMBs for Li^+ transport regulation^[49,50]. In these confinement channels formed by uniform nanopores of porous structures, Li^+ can be partially or completely desolvated [Figure 8B] as long as the pore size is smaller than solvent molecular size^[51]. This sieving layer dramatically reduces the desolvation energy and boosts Li^+ fast migration at interphase, hence effectively suppressing dendrites formation.

Based on the above concepts, a series of ionic conductors based on sieving layer have been developed. For example, Chang *et al.* reported MOF films soaked with 1 M propylene carbonate (PC)-LiTFSI solution as ionic conductors to replace conventional separators and electrolytes^[51]. This ionic conductor exclusively contains the solvent-depleted CIP ion pairs since the solvent molecules have been peeled off before entering into MOF film. However, only PC molecules accompany Li^+ penetrating into MOF pores due to the similar size (0.65 nm). The developed electrolyte displayed a significantly increased electrochemical stability window (4.5-5.4 V vs. Li/Li^+), as well as improved stability to NCM-811 cathodes^[51]. Certainly, MOFs can also be used to modify separators for binding these anions and solvent molecules through their unique pore

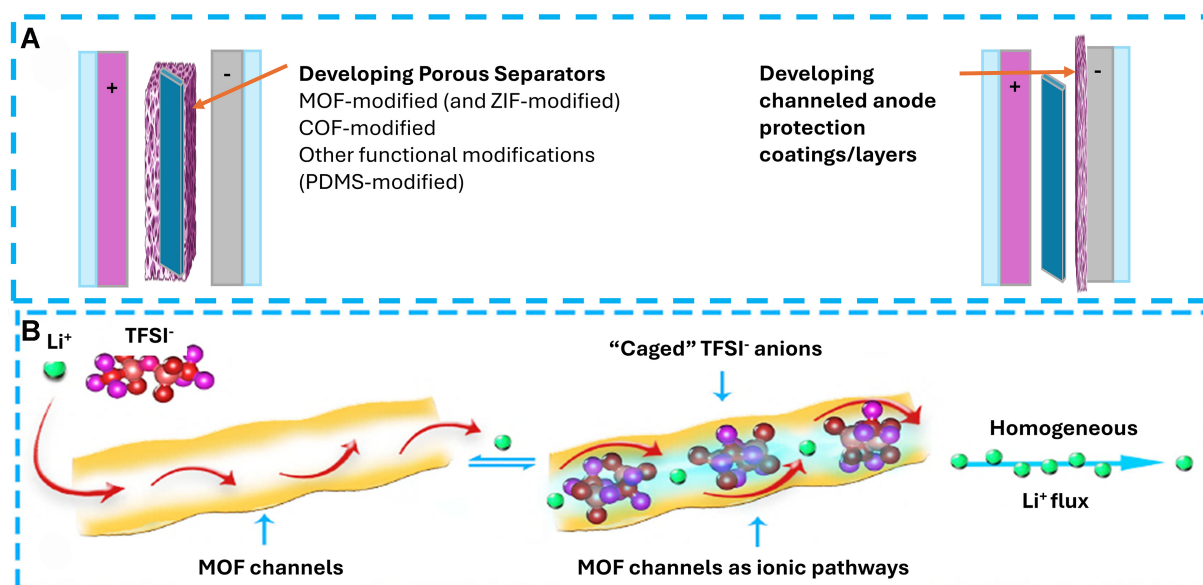


Figure 8. (A) Schematic representation of using porous membrane structures such as MOF, ZIF, COF, and others to favor desolvation and improve the Li^+ transport kinetics at interface; (B) The selective Li^+ transport while locking up the other species within the pores caused by the typical MOF channel is depicted graphically. Reproduced with permission^[50]. Copyright 2018, Elsevier. MOF: Metal-organic framework; ZIF: zeolitic imidazolate framework; COF: covalent organic framework.

size, thus resulting in a high Li^+ transference and uniform flow^[52]. For example, Li *et al.* designed a MOF coating layer on conventional separators, but different from the above MOF modification, these MOF particles are bridged with nitrogen-doped carbon (MOF@CC). As large-sized solvated Li^+ ions pass through the small channels of this MOF@CC layer, the outer solvation sheath of the complex can be sieved, and the active C-N bridging bond in MOF@CC functioned as a catalytic site to drive the desolvation of inner $\text{Li}(\text{solvent})_x^+$ with the aid of quick electronic injection facilitating the fast generation of naked Li^+ ions in L/S batteries. To cope with the slow sulfur/sulfide reaction rates in Li/S batteries, the as-prepared MOF with catalytic functionalities is sought to also improve the lithium polysulfide (LPS) conversion kinetics. In bulk solution, Li^+ ions surrounded by organic ether solvents impede the redox conversion between sulfur species. The solvation structure of Li^+ transforms into anion-derived modes such as AGGs and CIPs. These AGGs and CIPs increased the rate of Li^+ diffusion, preventing the formation of LPSs. The MOF@CC@PP modified cell shows higher capacities compared to the PP-based cell. Remarkably, the large areal pouch cell could maintain a capacity of $855 \text{ mAh}\cdot\text{g}^{-1}$ after 70 cycles^[53].

As shown schematically in Figure 9A, the confining electrolyte within the UiO-66-MOF channels induces partial desolvation of Li^+ , lowering the activation energy barrier for charge transfer^[54]. Moreover, benefiting from the chemical bonding interaction (confirmed by binding energy calculation by DFT) between Lewis acidic sites of MOF and anions, this MOF-modified electrolyte results in a high diffusion coefficient ($3.23 \times 10^{-7} \text{ cm}^2\cdot\text{s}^{-1}$) and a high t_+ (0.59), substantially suppressing the uneven Li deposition. Additionally, these MOF coatings on cathodes can also be beneficial in optimizing the Li^+ solvation structure. Chang *et al.* Designed a novel “ Li^+ de-solvated ether electrolyte” by mechanically coating a ZIF-7 MOF layer on NCM811 cathode^[55]. After cycling, the “ Li^+ de-solvated electrolyte” has a unique CEI layer on NCM811 surface. Li *et al.* prepared strong anion-shielding MOF-based composite interlayers on the anode in combination with polyvinylidene fluoride-hexafluoropropylene copolymer to attain high Li^+ transference number and homogeneous Li deposition due to the facile desolvation of Li^+ [Figure 9B]^[56].

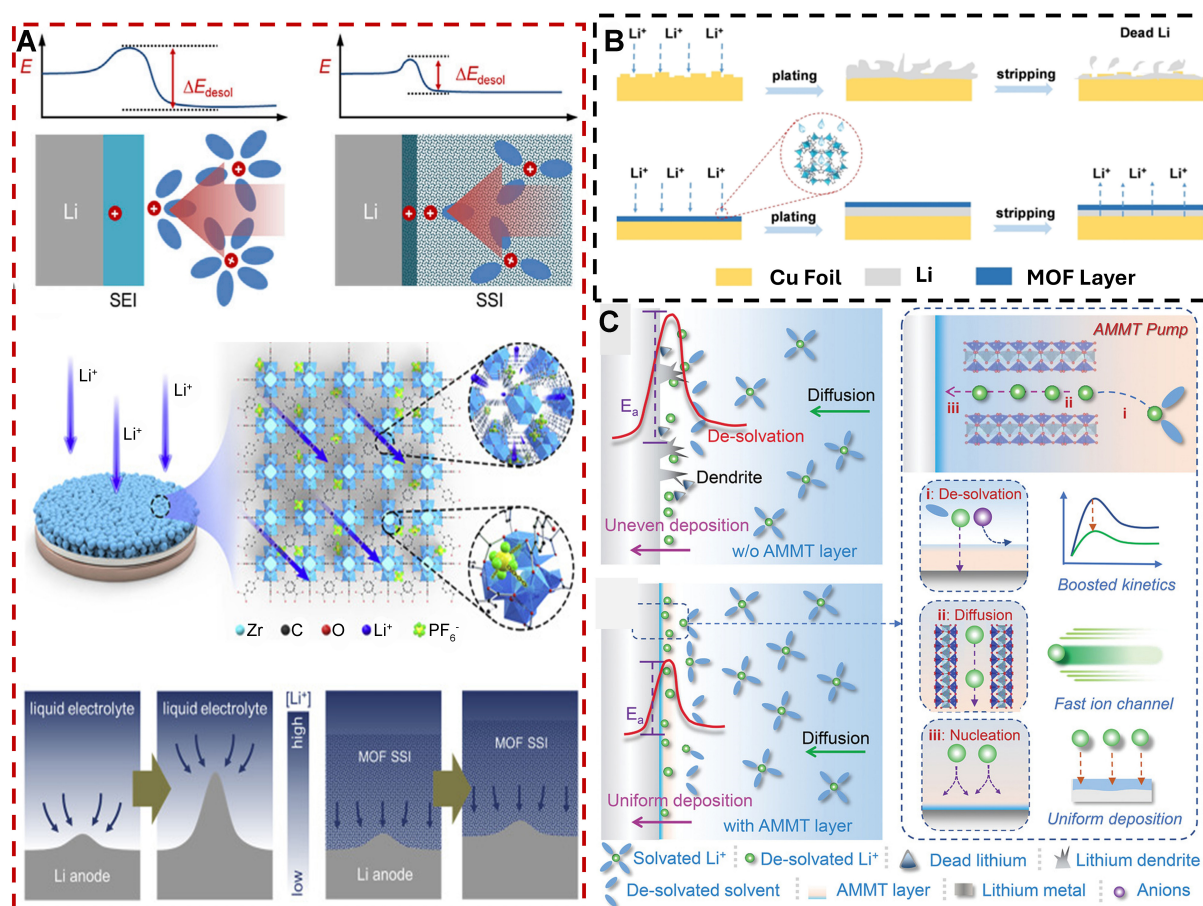


Figure 9. The Li⁺ desolvation is depicted schematically by channeled/porous layers on anode for fast Li⁺ transport and uniform deposition mechanism. (A) Li⁺ desolvation in liquid electrolyte and MOF-based SSI developed on LMA with immobilized anions interacting with Lewis acidic sites of pores and ionic channels for rapid Li⁺ transport. Li⁺ flow (arrows) and concentration (grayscale) along the LMA surface, as well as Li deposition morphology with and without MOF-based SSI, are shown. Reproduced with permission^[54]. Copyright 2020, Elsevier; (B) The behavior of Li plating/stripping on naked Cu foil and MOF-interlayer@Cu foil. MOF is responsible for desolvation, the rapid Li⁺ transfer and uniform flow, resulting in a smooth Li deposition. Reproduced with permission^[56]. Copyright 2022, WILEY-VCH; (C) A pure lithium-metal anode has poor desolvation and a lithium anode with an AMMT layer has a low desolvation barrier resulting in simplified desolvation. Reproduced with permission^[48]. Copyright 2023, WILEY-VCH. MOF: Metal-organic framework; SSI: semi-solid interphase; LMA: lithium metal anode; AMMT: Ag-montmorillonite.

COF materials with -OH functional groups may form hydrogen bonds with electrolyte solvents, which may regulate the desolvation process. For example, Yang *et al.* developed 2,4,6-trihydroxy-1,3,5-benzenetricarboxaldehyde (TPB)-4,4'-diamino-[1,1'-biphenyl]-3,3'-dicarboxylic acid COF membrane [TPB-BD(OH)₂-COF]-modified separators to create plenty of hydrogen bonds, such as OH...F (in OH/PF₆), OH...O (in OH/EC), and OH...O [in OH/ethyl methyl carbonate (EMC)]. Benefiting from these hydrogen bonds, the overwhelming number of free solvent molecules in the Li⁺ solvation sheath is reduced, hence leading to the easy desolvation process, while forming more aggregative structure for fast Li⁺ migration in bulk electrolyte. The full cell built with a COF-modified separator demonstrates superior cycling stability and even works functionally under extreme conditions (-60 °C)^[57]. A cationic COF comprised of positively charged organic moieties and weakly linked fluoride anions (F⁻) has been reported to modify the commercial polypropylene separator to form (COFF@PP). It was discovered that the organic units have an abundance of nanopores which homogenized the Li⁺ flux, and interaction between the solvent molecules and organic units of COFs reduced the degree of Li⁺ solvation structure resulting in a simpler desolvation of

Li^+ thus increasing the mobility rate. COF-DEC has a roughly threefold greater interaction energy than Li^+ and DEC, indicating that the COF units would compete with Li^+ for solvent molecules and bind them around the separator to simplify the Li^+ desolvation structure. Furthermore, the F^- inside the nanopores has been shown to aid in the construction of a strong LiF -rich SEI to avoid parasitic reactions between LMA and electrolyte^[49]. The chemical bonding strategy can also be applied in a cationic COF with positively charged organic moieties, which can form weak interaction with fluoride anions (F^-). The anchored anions result in a simpler desolvation of Li^+ thus increasing the mobility rate. From an absorption perspective, it has been calculated that COF-DEC has a roughly threefold greater interaction energy than Li^+ and DEC, indicating that the COF units would compete with Li^+ to interact with solvent molecules and bind them around the separator to simplify the Li^+ desolvation structure^[52].

Development of catalytic modulation layer for desolvation

Some catalytic protection layers or artificial SEIs have recently been noticed to encourage the desolvation process, too. Multiple lithiophilic hotspots in artificially produced LiNO_3 -rich layers, for example, readily promoted desolvation resulting in well-distributed surface adsorption prior to deposition. The underlying process is the enhanced capacitive adsorption of Li^+ ^[58]. The electrical interaction between the solvated Li^+ and the defect-based catalysts can significantly reduce the Li^+ -solvent chemical binding, allowing for quicker desolvation^[13].

Pure Li foils can absorb organic solvents from electrolytes raising the energy barrier for desolvation and nucleation. According to extensive spectroscopic, simulation, and electrochemical analyses, lithiophilic or catalytic artificial layers could also reduce the LMA surface affinity towards solvent molecules and significantly homogenize the lithium atoms flow for lateral deposition lowering the desolvation and nucleation barriers^[59,60]. For the artificial SEI, Feng *et al.* constructed an AMMT-based inherent channel with a negative charge layer on nanosheets. Combined with lithiophilic cations (such as Mg^{2+} and Ag^+) exchange and exfoliation, the prepared layer acted as an ion-rectifying pump, offering intrinsic rapid Li^+ transfer pathways. Directly dissociating solvated Li^+ from the solvent molecules due to the strong coulombic force considering the negatively charged layers of AMMT-SEI results in a lower desolvation barrier [Figure 9C]^[48].

Wang *et al.* reported a catalytic kinetic layer that acted as a promoter to bind atomic iron to cationic vacancy-rich 3D porous carbon^[61]. Free Li^+ ions are electrocatalytically dissociated from the Li^+ solvation structure for uniform lateral diffusion by lowering desolvation and diffusion barriers via a catalytic layer, resulting in smooth dendrite-free Li plating [Figure 10A and B]. In another study, Wang *et al.* reported highly active single metal cobalt anchored in a vacancy on hierarchical porous nanocarbon^[62]. Several atomic sites, serving as an artificial protective modulation layer on the lithium surface, demonstrate superiority in modifying Li^+ transport behaviors and smoothing the lithium deposition [Figure 10C and D].

Clamp-like coordination structure of polyethylene oxide (PEO)-based electrolytes causes a crowding of the solvation sheath and excessively strong chemical bonding interaction between electrolytes and Li^+ , making it difficult to dissociate free Li^+ . Wen *et al.* investigated their weakly solvating properties via the control of coordinating geometry. The unique distorted asymmetry helical solvation sheath efficiently reduced Li^+ -electrolyte binding, resulting in accelerated Li^+ desolvation kinetics, changed interfacial chemistry, and improved the performance at room temperature^[63]. To truly comprehend the charge-transfer behavior, a more sophisticated understanding of the chemical bonding interaction between solvation structure, interphase content, and corresponding ion dynamics, along with modern experimental analytical techniques at the interphase, is required.

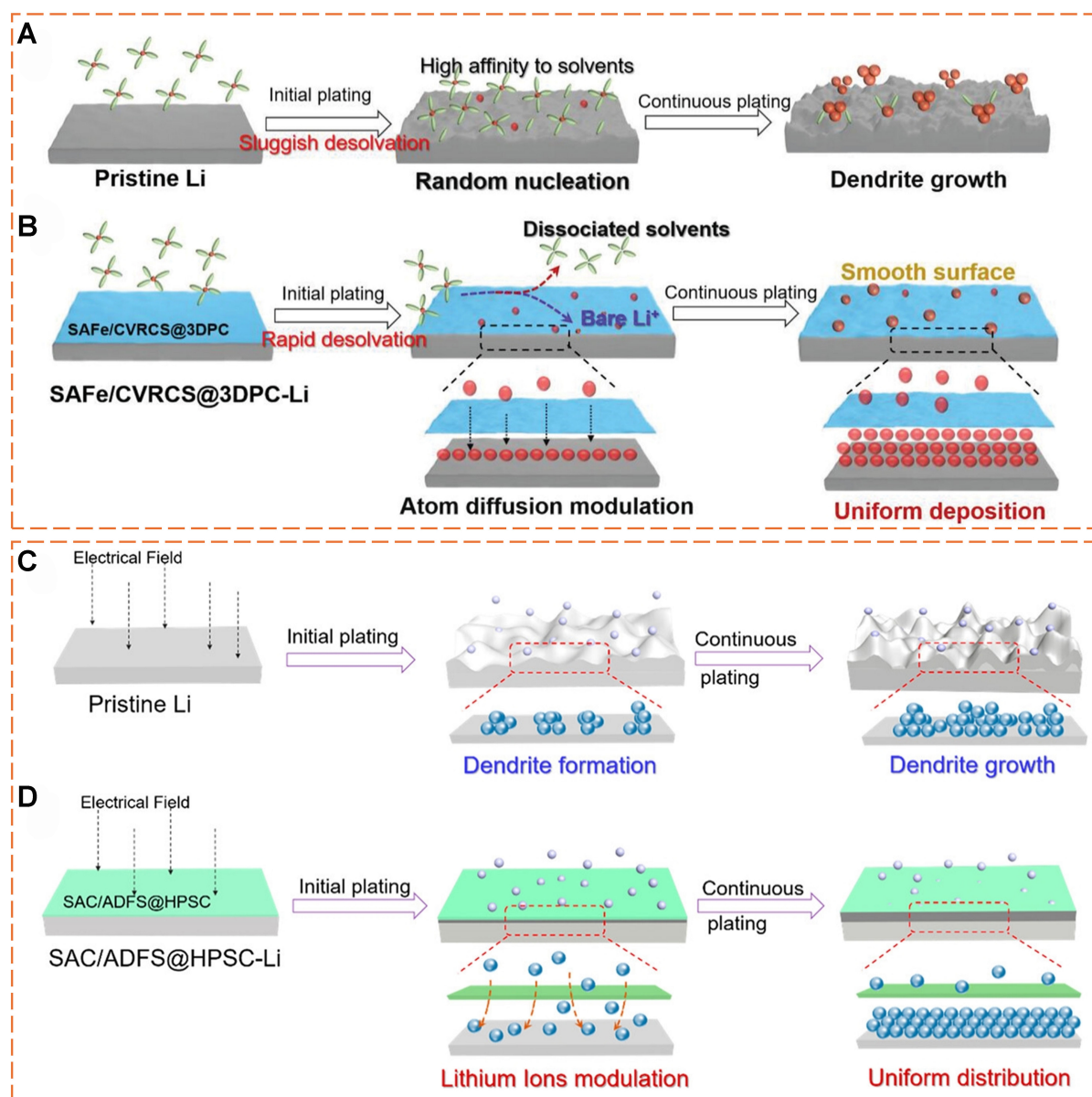


Figure 10. Schematic representation of (A) Li plating on pristine LMA with sluggish desolvation and (B) Li plating on SAFe-based catalytic surface with facile interfacial Li⁺ desolvation. Reproduced with permission^[61]. Copyright 2023, WILEY-VCH; Schematic representation of (C) plated Li on pristine Li and (D) Plated Li on SACo/ADFS@HPSC catalytic layer with fast Li⁺ transport. Reproduced with permission^[62]. Copyright 2021, American Chemical Society. LMA: Lithium metal anode.

Tailoring the electrolyte solvation towards conductive and stronger SEI

The “interface” between the electrode and electrolyte in LMBs is where electrochemical reactions and electron exchange occur. In the case of highly reversible electrochemical reactions, the ideal “interface” thickness should be zero. However, irreversible side reactions of the electrolyte at the electrode surface led to the formation of a SEI layer, which creates a new “interphase” between the electrode and electrolyte^[64]. Although extensive research has been conducted on the composition, structure, and advanced construction of artificial SEI layers, relatively more focus has recently been placed on the tailoring of electrolyte solvation structure and the SEI layer. In fact, the solvation structure of the electrolyte determines the function of the SEI layer to a certain extent^[65]. This section will elucidate the formation of organic, inorganic, and hybrid

organic/inorganic SEI from the perspective of solvation structure and their functions in improving the kinetics of Li^+ ion transport [Table 1].

Organic SEI layer

The use of EC in electrolytes has successfully opened the door to commercial LIBs. Understanding the decomposition products of EC molecules is the starting point for researchers to realize the organic component of the SEI. Fong *et al.* identified EC as a key solvent in the formation of SEI, but its reductive decomposition products have not been confirmed^[66]. Previously, the organic component in SEI was believed to be lithium ethylene di-carbonate (LEDC), which was formed via a single-electron charge transfer reaction of EC at around 0.8 V [Figure 11A]. Wang *et al.* synthesized lithium ethylene mono-carbonate (LEMC) and lithium methyl carbonate (LMC) through a simple and high-yield way, and measured ionic conductivity of LEMC as $0.006 \text{ mS}\cdot\text{cm}^{-1}$, which is a good ionic conductor [Figure 11B and C]^[67]. In contrast, LEDC and LMC are almost ionic insulators, and LEDC is highly reactive and unstable in batteries. As the main organic component in SEI, LEMC ensures the rapid transfer of Li^+ ions.

Chu *et al.* conducted systematic research of the relationship between SEI and the solvation structure at different concentrations of 0.1–1.0 M LiTFSI in DOL/DME [Figure 11D]^[21]. In low-concentration systems, Raman spectra [Figure 11E] showed that there are many free solvent molecules, and the preferential decomposition of the solvent results in the presence of a large number of organic species in the SEI components, leading to poor cycle performance of Li/Li and Li/Cu cells at different current densities.

High elastic modulus design is an effective method to improve the compatibility of the organic SEI layer and the volume effect of electrode materials during the charge and discharge process of LMAs. Hu *et al.* designed the 1 M LiTFSI in vinylene carbonate (VC) electrolyte that generates a stable and highly conductive SEI on the LMAs^[68]. X-ray photoelectron spectroscopy (XPS) analysis revealed that the SEI layer has a high carbon content on the surface and the F element remains relatively stable throughout the SEI. This indicates that VC plays a crucial role in the initial stage of reduction polymerization to form the organic SEI, which stabilizes the LMAs [Figure 11F]. Li/Li symmetric cells can maintain stable plating and stripping for 4,000 h, even at a high current density of $5 \text{ mA}\cdot\text{cm}^{-2}$ and an areal capacity of $10 \text{ mAh}\cdot\text{cm}^{-2}$ [Figure 11G]. However, most organic SEI components still have drawbacks such as low Li^+ ions conductivity and poor interfacial stability. Overall, the single organic SEI component is still not the optimal choice for stable LMBs.

Inorganic SEI layer

Compared with the organic SEI layer, the inorganic-rich SEI layer has excellent ionic conductivity and electronic insulation^[27]. Moreover, the high Young's modulus of the inorganic SEI layer can also suppress the growth of lithium dendrites. This section will discuss the construction strategies of inorganic SEI components from a coordination chemistry perspective, including LiF, LiCl, Li_3N , and hybrid inorganic components. With LiF as the main component, the fluorinated SEI can improve the cyclic stability of LMAs and facilitate the uniform plating/stripping^[69]. LiF-rich SEI can be produced in high-concentration electrolytes containing abundant FSI^- or bis(trifluoromethanesulfonyl)imide (TFSI⁻) anions. Additives such as FEC and di-fluoroethylene carbonate (DFEC) are also commonly used to construct fluorinated SEI. Xie *et al.* designed fluorinated molecules to promote the formation of LiF to construct stable and conductive SEI. The C–F bond on a perfluoro chain ($-\text{CF}_2-\text{CF}_2-$) has a high binding energy and is difficult to break during electrochemical reactions^[70]. The β -position of 2,2,3,3-tetrafluoro-1,4-dimethoxybutane (DFA) molecules contains an inert methoxy group ($\text{H}_3\text{CO}-$), which cannot undergo a defluorination progress. By introducing NO_3^- functional groups at the β -position, all the F atoms can be effectively released into 2,2,3,3-

Table 1. The advantages and disadvantages of SEI with different components

SEI components	Advantages	Disadvantages
Organic layer	Compatible with volume effects High flexibility Good interface contact	Poor mechanical strength Low Li ⁺ conductivity Electrochemical instability
Inorganic layer	High Li ⁺ conductivity High mechanical strength High electronic insulation	Fragile Poor flexibility Weak interfacial contact
Hybrid organic/inorganic layer	Excellent Li ⁺ conductivity Good electrochemical stability Balancing flexibility and rigidity	Uncontrollable composition and structure

SEI: Solid electrolyte interphase.

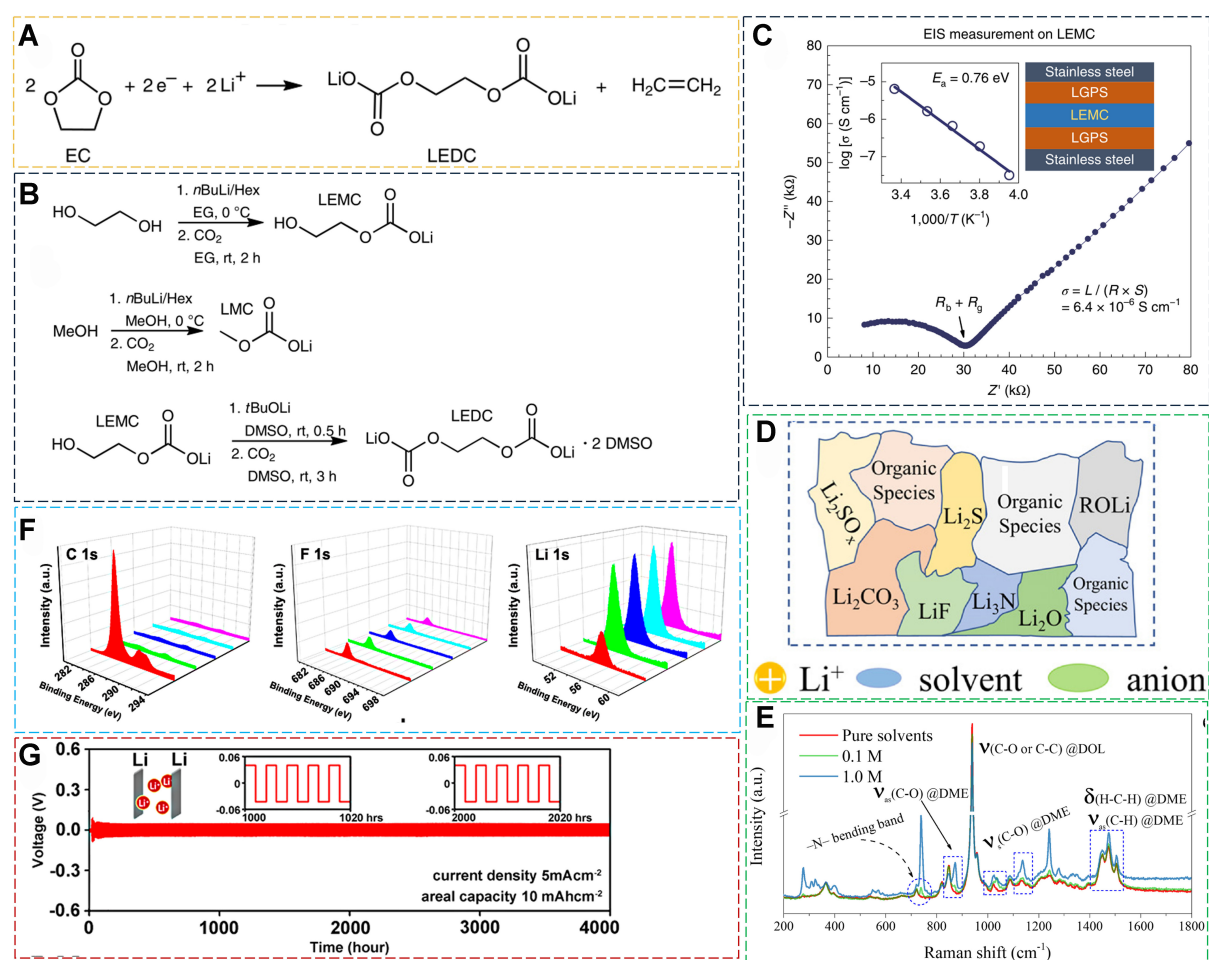


Figure 11. (A) The EC reduction via a single-electron pathway. Reproduced with permission^[67]; (B) Chemical synthesis of LEMC, LMC and LEDC-2DMSO. Reproduced with permission^[67]; (C) The ionic conductivity measurement of LEMC. Reproduced with permission^[67]. Copyright 2019, Springer Nature; (D) The schematic illustration of SEI layer with organic species. Reproduced with permission^[21]. Copyright 2023, Elsevier; (E) Raman spectra of electrolytes with different salt concentrations (LiTFSI in DOL/DME) and the schematic illustration of SEI layer with organic species. Reproduced with permission^[21]; (F) XPS analysis spectra of C 1s, F 1s, and Li 1s of the SEI. Reproduced with permission^[68]; (G) Li/Li symmetrical cell cycled under a current density of 5 mA cm^{-2} and an areal capacity of 10 mA h cm^{-2} . Reproduced with permission^[68]. Copyright 2018, American Chemical Society. EC: Ethylene carbonate; LEMC: lithium ethylene mono-carbonate; LMC: lithium methyl carbonate; LEDC: lithium ethylene di-carbonate; DMSO: dimethyl sulfoxide; SEI: solid electrolyte interphase; LiTFSI: $\text{Li}[\text{CF}_3\text{SO}_2)_2\text{N}]$; DOL/DME: 1,3-dioxolane/1,2-dimethoxyethane; XPS: X-ray photoelectron spectroscopy.

tetrafluorobutane-1,4-diol dinitrate (AFA) molecules. The elimination reaction at the β -position can activate the C–F bond and further induce the removal of the F atoms [Figure 12A]. In addition, the hydrofluoroether (HFE) has been shown to be an effective diluent in previous localized high-concentration electrolyte (LHCE) designs. As demonstrated in Zhang's work, fluorinated alkyls ($-\text{CF}_2-\text{CF}_2-$) are difficult to release F and construct LiF-rich SEI in LMAs. Tu *et al.* proposed the synergistic effect of diluents and anions in regulating the solvation structures and constructing SEI^[5]. The aromatic compound 1,2-dfBen was introduced as a diluent into the Pyr₁₃FSI ionic liquid electrolytes (ILEs) dissolving LiFSI. This 1,2-dfBen in ILE not only intensifies the interaction between Li⁺ and FSI, achieving an ultra-high proportion of AGGs in the solvation structure, but also participates in constructing LiF-rich SEI. The diluent reduces the viscosity of the ILE system and greatly improves Li⁺ transport kinetics in the bulk electrolyte and the interface. It was revealed that the specific coordination mode is the enhancement of the coordination between Li⁺ and the O atom on the side of the N atom. This extends the concept of LHCE and rational optimization of diluents [Figure 12B]. Similarly, Zhu *et al.* proposed two other aromatic compound diluents, trifluoromethoxybenzene (TFMB) and benzotrifluoride (BZTF), which have a synergistic effect with anions to promote the formation of uniform and stable LiF-rich SEI [Figure 12C]^[71]. Different from LiF, the chlorine-doped double halide SEI ($\text{LiF}_{1-x}\text{Cl}_x$) has faster Li⁺ ions conductivity^[72]. As shown in Figure 12D, the energy barrier for Li⁺ ions to migrate in $\text{LiF}_{1-x}\text{Cl}_x$ is significantly lower than that in LiF under the same migration pathway^[73]. The Cu/NCM523 pouch cell with 1.3 M LiFSI in DME/DCE (1,2-dichloroethane) provides 70% capacity retention after 125 cycles.

The Li₃N is a common component of inorganic SEI and exhibits superior ionic conductivity compared to LiF. Adding LiNO₃ to carbonate or ether electrolyte systems is the simplest and most widely used way to construct Li₃N-rich SEI. However, NO₃[−] has a high DN value (22) and the strong interaction between Li⁺ and NO₃[−], resulting in a low solubility. Liu *et al.* dissolved large amounts of LiNO₃ using dimethyl sulfoxide (DMSO) (DN value of 30), and then added the complex (LiNO₃-S) into LiPF₆ FEC/DMC electrolyte^[74]. After the addition of LiNO₃-S, the solvation sheath structure of Li⁺ ions transforms from FEC and DMC molecules to NO₃[−], forming a Li₃N-rich SEI. The morphology of lithium deposition also changes from a loose dendritic structure to a dense block shape [Figure 13A]. In addition to using solvents with high DN values to dissolve LiNO₃, Zhang *et al.* reported Sn²⁺ and In³⁺ as the Lewis acids to increase the solubility of LiNO₃ in carbonate electrolyte, greatly improving the cycling stability of LMBs^[75]. However, the influence of these multivalent metal cations on the SEI may be related to specific adsorption of inner Helmholtz plane (IHP). Yan *et al.* found that trace amounts of Cu²⁺ reached the lithium metal interface and then NO₃[−] anions, as the main solvation sheath of Cu²⁺, were carried to the IHP, inducing the formation of Li_xO_y-rich SEI and promoting the spherical lithium metal deposition [Figure 13B]^[76]. Wang *et al.* designed a novel amide-based electrolyte 1 M LiTFSI in 2,2,2-Trifluoro-N,N-dimethylacetamide (FDMA)/FEC (1/1 by vol.), which also formed Li₃N-rich SEI through solvent optimization. The N-CH₃ bond in FDMA is attacked by two Li⁺ and two electrons, eventually forming Li₃N-rich SEI^[77]. Research shows that the hybrid inorganic SEI components often exhibit superior performance. By combining the rapid Li⁺ ion transport kinetics of Li₂CO₃ with the excellent electron insulation properties of LiF, Wu *et al.* developed tris(4-fluorophenyl)phosphine (TFPP) as an electrolyte additive to construct a Li₂CO₃/LiF heterostructured SEI^[78]. The heterostructured SEI exhibits the highest Li⁺ ion affinity (0.66 eV), which facilitates uniform Li⁺ ion flow and enables rapid diffusion of Li⁺ ions in the SEI [Figure 13C]. Recently, Mao *et al.* reported an anion-enrichment interface, which is achieved by using weakly dissociated lithium salts [LiBF₄ and lithium difluoro (oxalate) borate (LiDFOB)] and ethyl 3,3,3-trifluoropropanoate (tFEP). Anion enrichment at the interface promotes further decomposition of anions, forming an SEI layer rich in various inorganic substances [Figure 13D]. In the designed electrolyte, the energy barrier for Li⁺ ion migration through the SEI is 25.89 kJ·mol^{−1}, which is lower than 36.58 kJ·mol^{−1} of the commercial electrolyte^[79]. The impact of Li₂O-rich SEI on CE has been recently revealed, demonstrating the possibility of achieving CE higher than 99%

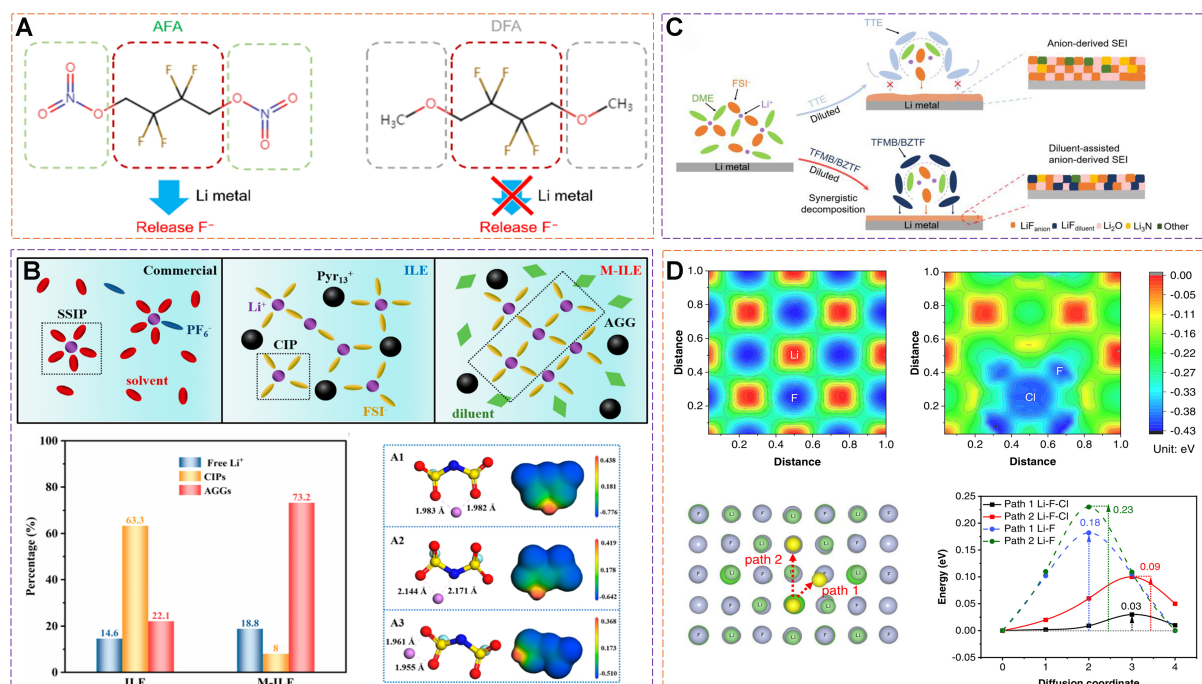


Figure 12. (A) Molecular structure of AFA and DFA. Reproduced with permission^[70]. Copyright 2022, WILEY-VCH; (B) The schematic illustration and Raman spectra of M-ILE and three types of Li-FSI⁻ coordination. Reproduced with permission^[5]. Copyright 2022, American Chemical Society; (C) The schematic diagram of synergistic function between diluents and anions. Reproduced with permission^[71]. Copyright 2022, American Chemical Society; (D) The energy barrier of migration pathway of LiF and LiF_{1-x}Cl_x. Reproduced with permission^[73]. Copyright 2022, Springer Nature. AFA: 2,2,3,3-tetrafluorobutane-1,4-diol dinitrate; DFA: 2,2,3,3-tetrafluoro-1,4-dimethoxybutane; ILE: ionic liquid electrolyte.

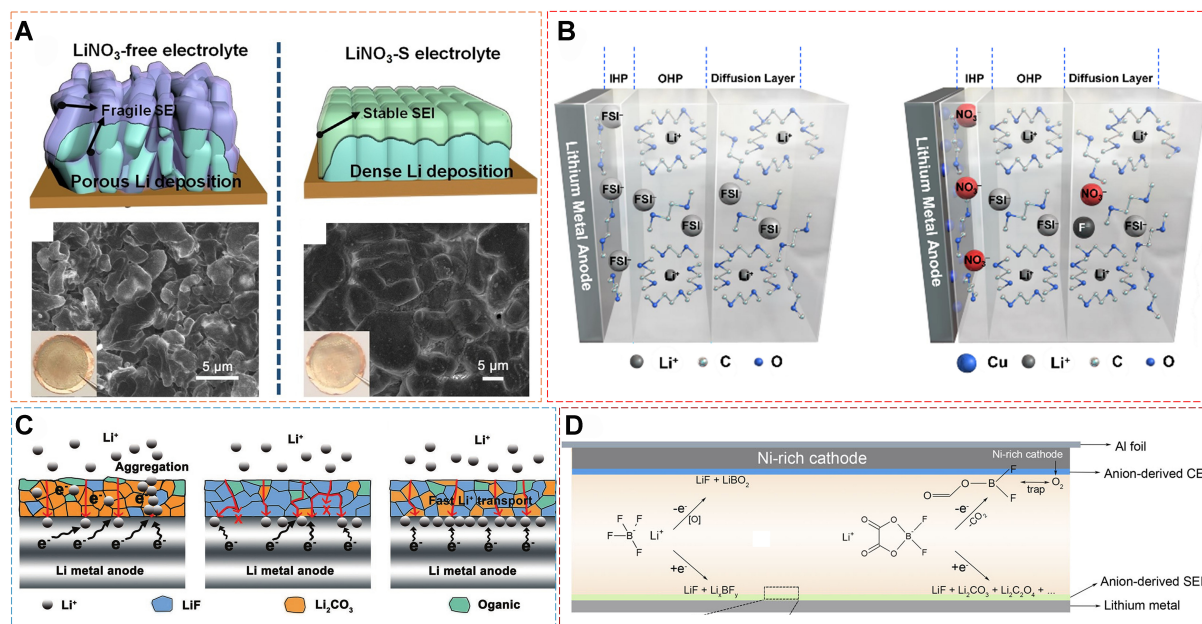


Figure 13. (A) Li morphology deposited on Cu foil with LiNO₃-free and LiNO₃-S electrolyte. Reproduced with permission^[74]. Copyright 2020, WILEY-VCH; (B) Schematic illustration of adsorption characteristics with different ions in IHP and OHP. Reproduced with permission^[75]; (C) The heterostructured SEI exhibiting the highest Li⁺ ions affinity. Reproduced with permission^[78]. Copyright 2022, WILEY-VCH; (D) Schematic illustration of anion-enrichment interface. Reproduced with permission^[79]. Copyright 2023, Springer Nature. IHP: Inner Helmholtz plane; OHP: outer Helmholtz plane; SEI: solid electrolyte interphase.

using oxygenated rather than fluorinated solvents and salts to obtain highly competitive SEI^[80]. Therefore, the combination of multiple inorganic substances in the inorganic SEI layer has greater potential to stabilize LMAs and promote fast Li⁺ ion transport kinetics.

Robust hybrid organic/inorganic SEI layer

The inorganic SEI layer with high Young's modulus shows the ability to inhibit the growth of lithium dendrites, but its rigid characteristics are not compatible with the volume effect of the electrode material, and repeated rupture and reconstruction accelerate the failure of the battery. The hybrid organic-inorganic composition of SEI not only preserves the rapid Li-ion conductivity of the inorganic component but also possesses the excellent flexibility of the organic component, significantly improving the cycling stability of LMAs. Therefore, a polymer-in-salt electrolyte (PISE_{0.7}-TTE₉₀) has been developed using a highly concentrated LiTFSI as the salt, polyethylene glycol dimethyl ether (PEGDME) as the solvent, and TTE as the cosolvent^[65]. The time-of-flight secondary ion mass spectrometry (TOF-SIMS) results provide further insight into the dual-layer structure of the SEI formed in the PISE_{0.7}-TTE₉₀ system. The maximum intensity of the C₂HO⁻ signal is observed at the SEI surface, followed by rapid decay. Conversely, the maximum intensity of the LiF⁻ signal appears at 10 s, followed by a smooth decay, indicating the formation of LiF under the C₂HO⁻ layer. The 3D reconstruction images clearly demonstrate that the SEI is composed of organic compounds on the top layer and inorganic compounds on the bottom layer. The formation mechanism of dual-layered SEI has also been thoroughly investigated through frontier orbital theory. In the PISE_{0.7}-TTE₉₀ system, TFSI⁻ has a reduced lowest unoccupied molecular orbital (LUMO) than PEGDME molecules, resulting in its preferential decomposition into inorganic components on the LMAs. Then, PEGDME molecules are attacked by electrons to form radicals, which get self-polymerization to form a polyether network.

Organic-inorganic SEI can also be constructed using room-temperature ionic liquids (RTILs). Wang *et al.* immersed the LMAs in a reactive ionic liquid (Pyr₁₃FSI), where the highly reactive FSI⁻ anions react with LMAs to form an inorganic layer of LiF, and the organic segments were chemically adsorbed on the inorganic layer^[81]. Thus, a well-ordered organic-inorganic SEI layer can be obtained through a simple self-assembly approach [Figure 14A]. The atomic force microscopy (AFM) shows that the average roughness of the LMA surface was only 19 nm, and the Young's modulus of the organic and inorganic layers was further calculated from the force curve to be 2.1 and 25.19 MPa, respectively. Ionic liquids can effectively construct organic-inorganic dual-layer SEI due to their unique molecular structure. Wang *et al.* dissolved 0.1 M LiDFOB in N-methyl-N-methoxyethyl-pyrrolidinium bis(trifluoromethylsulfonyl)imide ([MEMP][TFSI]) ionic liquid with TTE as a co-solvent, developing an ultralow-concentration electrolyte (ULCE). Due to the lower LUMO value, Li⁺-DFOB⁻ and Li⁺-TFSI⁻ will preferentially decompose at the interface, ensuring the cycling stability of LMAs. Additionally, the surface protrusions of LMAs possess a higher potential, resulting in the migration of MEMP⁺ towards them under an electric field [Figure 14B]. The electrostatic repulsion effect between Li⁺ and MEMP⁺ will promote the formation of uniform Li⁺ ion flux and suppress the growth of lithium dendrites^[82].

Yan *et al.* have demonstrated that FEC can spontaneously form a dual-layered film on the surface of LMAs [Figure 14C]^[83]. The ab initio molecular dynamics (AIMD) analysis reveals that positive-charged Li atoms and negative-charged F atoms can break the C-F bonds in FEC through electrostatic attraction. As a result, organic compositions such as CH₂CHOCO₂Li and CH₂CHOLi deposit on the electrode surface, forming a dual-layered interface structure with an organic outer layer and an inorganic inner layer. The average Coulombic efficiency (CE) of Li/Cu cells can reach 98.3%, and the capacity retention of anode-free Cu/NCM523 cells remains at 67.7% after 20 cycles, and the morphology of the LMA is dendrite-free. Li *et al.*

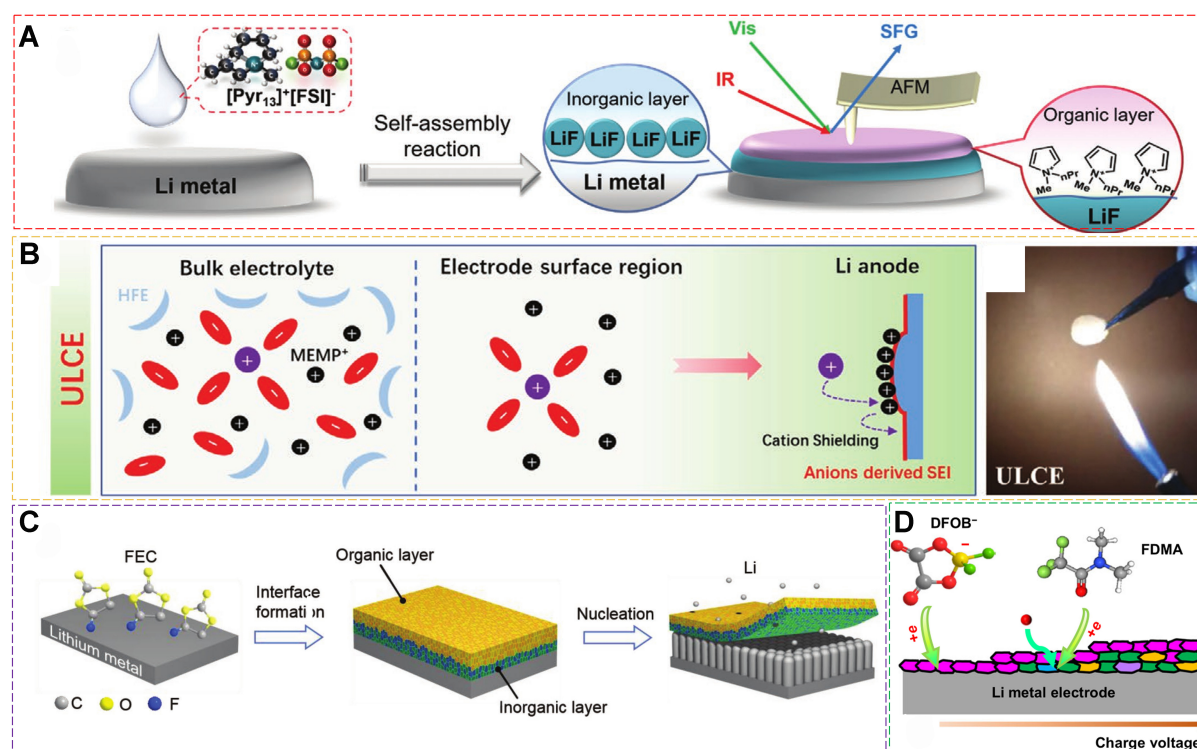


Figure 14. (A) The schematic synthesis of ordered SAHL SEI layer. Reproduced with permission^[81]; (B) Schematic illustrations of the solvation structure of ULCE. Reproduced with permission^[82]; (C) Organic/inorganic SEI dual-layer derived from decomposing FEC solvent. Reproduced with permission^[83]; (D) Schematic representation of the dual-layered SEI formed on the lithium metal electrode. Reproduced with permission^[84]. SAHL: self-assembled ordered organic/inorganic hybrid dual layers; SEI: solid electrolyte interphase; ULCE: ultralow-concentration electrolyte; FEC: fluoroethylene carbonate.

developed a quasi-solid-state polymer electrolyte with an ionic conductivity of $2.2 \times 10^{-4} \text{ S}\cdot\text{cm}^{-1}$ at -20°C by utilizing the self-polymerization of 1,3,5-trioxane (TXE). The co-decomposition of DFOB⁻ anions and FDMA produced a dual-layer SEI with a dominating outer layer of $\text{Li}_x\text{BO}_y\text{F}_z$ and a LiF-rich inner layer [Figure 14D], which ensured the superior low-temperature performance of the polymer electrolyte^[84]. The activation energy for Li⁺ ion migration is calculated to be 0.33 eV, and the Li⁺ ion transference number is as high as 0.8 at -20°C . In summary, regulating solvent structure can be used to obtain SEI with different compositions. However, single-component SEI still has limitations in battery applications, such as poor interfacial compatibility, component fragility, and electrochemical instability. The organic-inorganic hybrid SEI layers have the advantages of high Li⁺ ion conductivity and robust mechanical properties. Understanding the intrinsic connection between solvent structure and SEI composition provides new opportunities for high-performance LMB design.

Kinetic modulation of hosts/current collectors

The interaction in Li–Li bonds is weaker than other metal bonds, such as Mg–Mg, which leads to a lower surface energy; thus, it is not surprising to observe Li deposition habit with low dimensional structure. To inhibit Li dendrites growth, delicate hosts with functions on reducing the diffusion energy barrier of lithium are quite necessary^[85]. In general, the diffusion energy barrier is associated with Li⁺ wettability of the host, Li⁺ mobility in the host and the current density of unit area in the host^[85]. As illustrated in Figure 15^[86], the essential characteristics of an ideal host/scaffold with improved Li deposition kinetics should include the following merits: (1) conductive network for better charge transfer and lower interfacial resistances; (2) abundant lithiophilic sites for decreasing the deposition overpotential or accelerating Li⁺ mobility; (3)

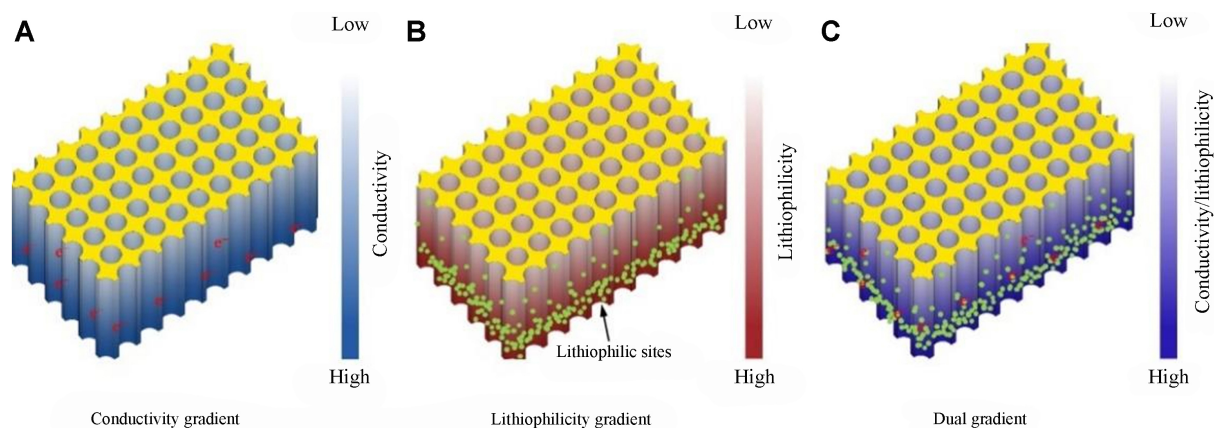


Figure 15. Lithium metal porous host design schematic. (A) electrical conductivity gradient; (B) lithium affinity gradient; (C) dual gradient. Reproduced with Permission^[86]. Copyright 2022, Science.org.

porous structure with high surface area for reducing the local current density^[85].

Host conductivity enhancement

Porous hosts with high conductivity and high surface area are expected not only to lower and uniformize the deposition current density through efficient coupling between electrons and Li^+ , but also to backstop the volume changes of plated Li, thus improving the deposition kinetics^[87]. Among various conducting materials, metal hosts, due to their superior conductivity, have been initially reported. These porous metal hosts (Ni, Cu, Ti, *etc.*) successfully bond with Li to reduce the deposition energy barrier. For example, Li *et al.* developed a copper mesh, which provides abundant deposition sites for Li plating. Compared to Cu foil as a current collector, this Cu mesh with large surface boosts electronic exchange, and simultaneously decreases the local current density; hence, superior plating stability can be observed^[88]. Although these porous metal hosts make some progress on improving Li cycle stability, it is still far away from the expectation of commercial application. The main reason is probably caused by the weak affinity between Li and metal hosts, which cannot support long lifespan of Li anodes^[89]. Moreover, the heavy weight of metal hosts is another negative factor for practical application in terms of cost and energy density. So, addressing these issues is still a big challenge.

Compared to heavy metal hosts, light carbon and its derivatives seem much more appealing due to their good conductivity^[90]. Nevertheless, because pure carbon materials are lithiophobic, Li dendrite development on carbon structures could be hampered by a large barrier to Li nucleation and uneven Li^+ distribution^[91]. Graphene, for example, has a low affinity for Li deposition/stripping (high overpotential). A lithiophilic medium is required to spatially guide and confine the Li deposition (bonding with Li^+) within the interior voids of porous carbon matrix^[92]. As a consequence, development of light hosts with lithiophilic properties seems necessary.

Lithiophilic modification of host

Lithiophilic modification enhances the affinity between Li and host material, and this increased bonding energy effectively reduces deposition energy barrier, thus suppressing dendrite formation. The larger binding energy between Li and the nucleation sites in the host, the easier lithium metal nucleation occurs on the host sites, well demonstrating Li deposition is a competitive process between lithium-lithium bonding and lithium-host bonding. Dopants, functional groups, and affinity coating layers have been normally introduced to a host for enhancing its lithiophilicity^[93].

The lithiophobic carbon host normally introduces dopants to modify its affinity with Li. For example, Wang *et al.* reported a graphene-based aerogel host with a Ag dopant (Ag@Graphene), which shows lower lithium deposition energy compared to a host without Ag, as evidenced by the lower Li nucleation overpotential^[92]. These Ag dopants dramatically increase the CE of Li/host in both carbonate and ether-based electrolytes with various capacities at different current densities. The reversible Li plating/stripping behavior can be attributed to the strong Li–Ag bonds, thus deriving a lower overpotential of Li deposition. In addition, heteroatom dopants also contribute to uniformly Li plating through the strong polar/polar interaction^[89]. For example, Br-doped graphene hosts boost Li transport kinetics through the strong Li–Br chemical bonds, which tremendously reduces Li nucleation energy barrier, acting as lithiophilic sites that facilitate rapid and uniform deposition [Figure 16]^[94].

Apart from dopants, affinity coating layers, such as SnSe, SnF₂, CuO, and so on, can also enhance the deposition performance of lithium. As illustrated in Figure 17A, SnSe–C affinity coating shows uniform Li plating behavior compared to a Sn–C layer due to the strong bonding energy in Li–Se. The Li/SnSe–C anode has an ultralong lifespan (over 1,100 h) and a low overpotential (18 mV)^[91]. The excellent performance can be contributed by the *in-situ* constructed Li₂Se with high ionic conductivity, which boots Li⁺ transport kinetics, enabling uniform Li⁺ deposition. Similarly, the CuO coating layer on Ti mesh also exhibits excellent ability on homogenization of Li⁺ flux by forming strong Li–O bonds, thus prolonging the Li anode lifespan [Figure 17B]^[95].

Based on the above results, it can be concluded that lithiophilicity is an important factor as conductivity for a host; therefore, balancing both two features in one host seems quite significant^[96]. Figure 17C–E depicts the influence of hosts with varying lithiophilicity and conductivity. A novel Cu current collector patterned with MoO₂–Mo₃N₂ heterojunction nanobelts mounted onto reductive graphene oxide is reported. The collector possesses synergistic functions of exceptional lithiophilicity, an integrated electric field generated by superb interfacial contact, and a thick lithiophilic SEI layer, which enables robust charge transfer and Li⁺ diffusion^[97]. All these results well demonstrate that a high-quality host should possess both conductive and lithiophilic features.

Kinetic modulation by catalysts on hosts

The lateral diffusion of Li is much slower than the vertical localized deposition rate. The major cause of this problem is the higher surface diffusion barrier and poor surface activity. How to efficiently reduce the surface diffusion barrier attracts the attention of researchers. Recently, researchers found that catalysts behave efficiently on modulating the Li diffusion kinetics at Li anodes^[89], especially single atom catalysts (SACs)^[98,99]. The active sites can be completely exposed when the size of these metallic modulators is reduced to atomic level, reaching 100% atomic efficiency^[62]. Controlling surface activation aids in increasing diffusion kinetics and achieving uniform deposition. In comparison to pure lithium metal with large diffusion barriers, adding SAC activators into the matrices results in a considerable drop of Li diffusion barrier down to 0.09 eV, thus increasing lateral diffusion for uniform plating^[89]. Single-atom Zn sites have been shown to drive high-dimensional lithium deposition kinetics, a lower migration barrier, a larger surface binding energy [Figure 18A], and rapid nucleation behavior, allowing for easy Li deposition. Li plating/stripping on Zn-single atoms (SAs) achieved low overpotentials of around 12 mV and a high CE of up to 100% [Figure 18B and C]^[99].

To reduce the Li nucleation barrier, SACs can be transplanted into several carbon matrices (graphene, MXene) to provide effective adsorbing and catalyzing lithiophilic sites. Several metal atoms supported onto nitrogen-doped graphene nanostructured matrices have been explored to govern their Li nucleation and

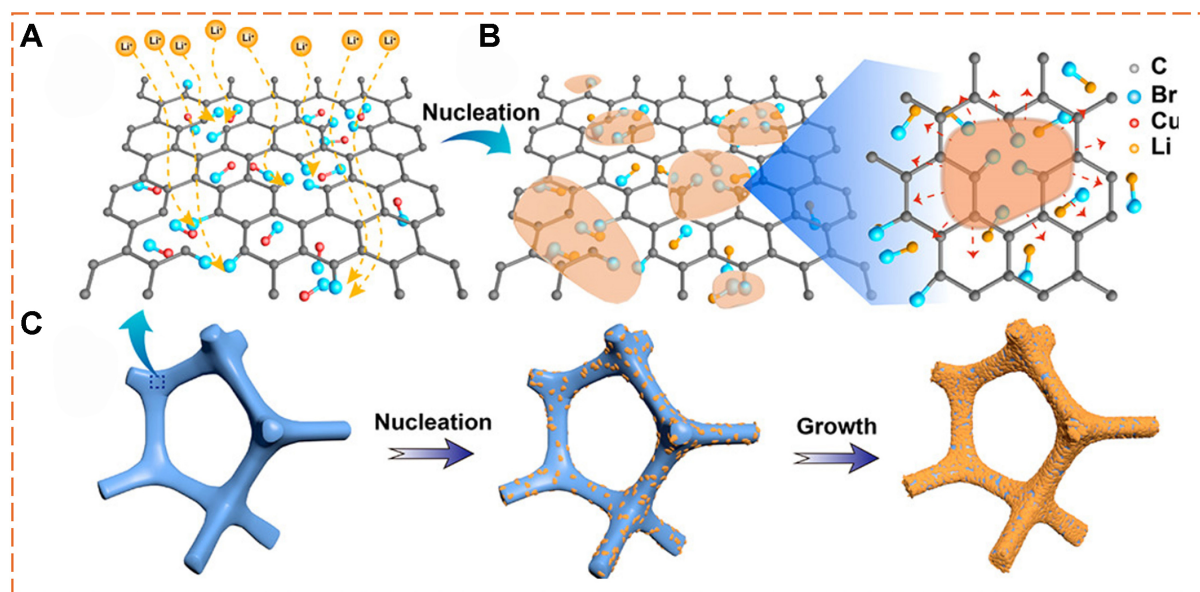


Figure 16. Illustration of lithium metal deposition on Br-doped graphene host. (A) Li^+ flow is homogeneous above Br-doped graphene-like sheet and CuBr; (B) CuBr was converted into LiBr after Li plating. The selective and targeted deposition of lithium metal on Br-doping sites, as well as the surrounding LiBr, govern lithium metal nucleation into Li seeds with a pancake-like shape. Gray, blue, red, and orange denote C, Br, Cu, and Li, respectively; (C) The nucleation and development of lithium metal on modified carbon host. Reproduced with permission^[94]. Copyright 2018, American Chemical Society.

deposition behaviors. By expanding the confined region, the higher concentration of SACs attached by nitrogen sites boosted the localized adsorption of Li atoms. Six kinds of SACs ($M = \text{Co}, \text{Mn}, \text{Zr}, \text{Ni}, \text{Zn}, \text{Cu}$) over N-doped graphene matrices have been examined for their lithiophilicity^[100]. Although single-atom zirconium (Zr) supported on a N-doped graphene matrix exhibited a higher predicted binding energy than other metals, it did not perform better in experiments. This means that the host requires a modest lithiophilicity for the Li to diffuse easily. The catalyst used to accelerate the Li^+ diffusion kinetics should have a modest affinity for Li^+/Li .

To effectively promote the Li growth and nucleation, single zinc atoms have been immobilized on MXene ($\text{Ti}_3\text{C}_2\text{Cl}_x$) layers. Owing to the excessive number of Zn atoms on the surface of Zn-MXene layers during the initial plating, Li tended to nucleate homogeneously and then expanded vertically along the nucleation sites, yielding bowl-like Li without dendrites. In contrast to graphene's converging electron density within chemical bonds, the addition of Zn-SAs assisted in delocalizing the electronic density throughout the whole plane, improving the electronic conductivity^[98]. Wang *et al.* proposed a conductive network encapsulating the most active SA cobalt on an anodic defect-containing iron sulfide in a hierarchically porous sulfur-doped nanocarbon, which acts as a kinetic modulation layer on the Li surface. The improved Li electrode reduces the nucleation barrier (15 mV) and greatly accelerates the Li horizontal deposition^[62]. Previous research has shown that pristine defect-containing or single atomic catalysts can provide catalytic sites to increase Li^+ kinetics.

The nucleation potential barrier for a Li atom has been reported to decrease from 225 to 29 mV at $1 \text{ mA}\cdot\text{cm}^{-2}$ upon experiencing the binary Ni and Fe metal atoms in ultralight N-doped carbon nanofiber paper (SAFeNi@LNCP) modulation layer. The smallest charge transfer resistance of the SAFeNi@LNCP-Li indicates the rapid electrochemical kinetics accelerated by the SACs^[101]. Figure 18D shows the mechanism of Li diffusion at a host with and without the SAC modulation layer on LMA. All these results well suggest the

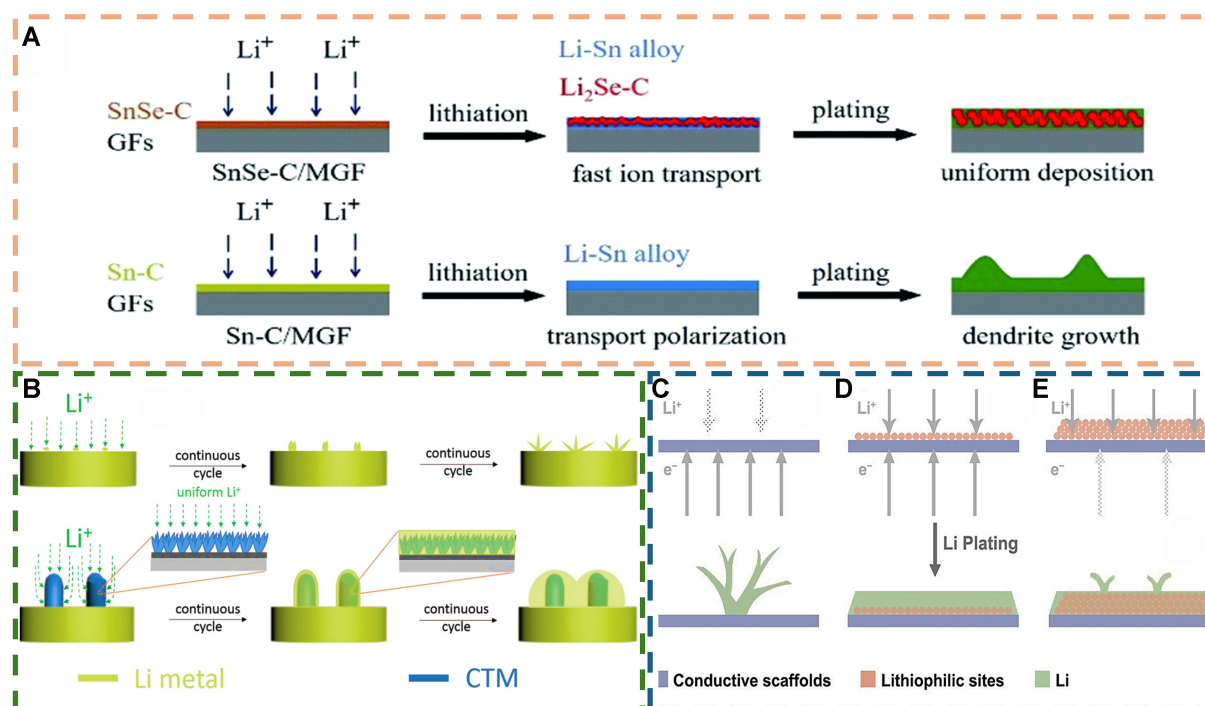


Figure 17. Schematics of Li deposition behaviors on lithiophilic modified scaffolds to regulate lithium nucleation and fast transport (A) on alloy SnSe-C/MGF scaffolds and Sn-C/MGF scaffolds. Reproduced with permission^[91]. Copyright 2013, Royal Society of Chemistry; (B) the Li plating behavior at bare Li wafer and a CuO@Ti-mesh CTM-based anode. Reproduced with permission^[95]. Copyright 2019, WILEY-VCH; (C) Li host of low lithiophilicity and high conductivity generated Li dendrites; (D) Li hosts with synergistic lithiophilicity, and conductivity showed homogeneous Li deposition and restricted Li dendrite development; (E) Host of high lithiophilicity and poor conductivity having high electrical resistance and inadequate for dendrite suppression. Reproduced with permission^[96]. Copyright 2020, WILEY-VCH. MGF: Modified glass fiber film; CTM: CuO@Ti-mesh.

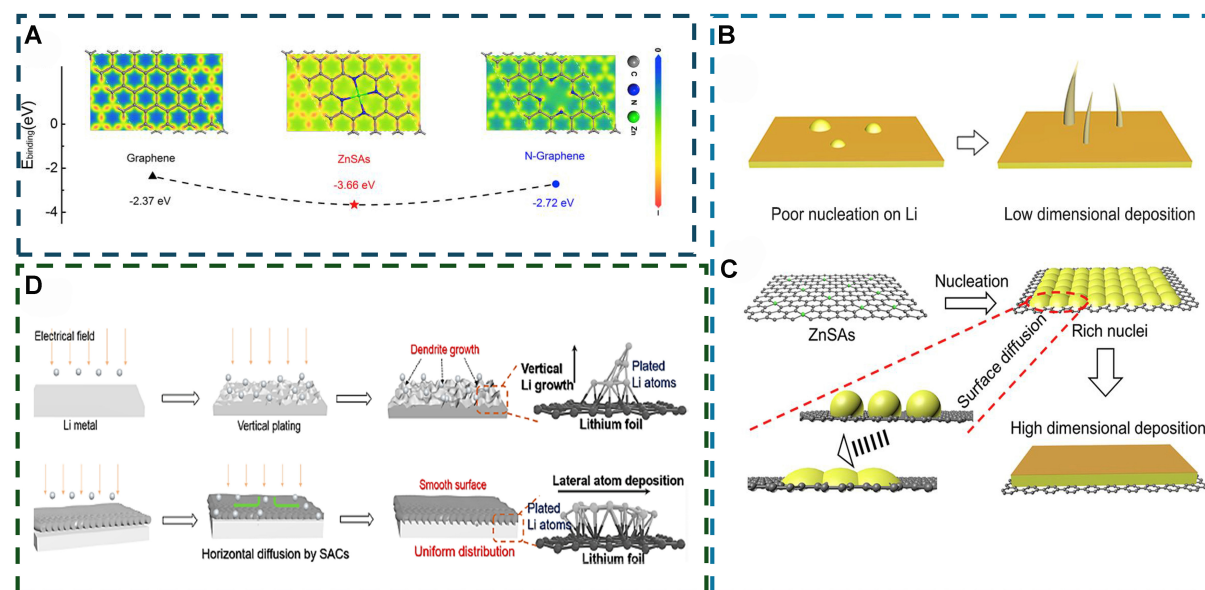


Figure 18. (A) Difference in electron density and surface binding energy between graphene, N-graphene, and ZnSAs; Lithium deposition behavior (B) on bare Li and (C) single-atom Zn sites. Reproduced with permission^[99]. Copyright 2019, Elsevier; (D) a mechanism of lithium atom diffusion on bare Li resulting in low dimensional vertical deposition (dendrites) and high dimensional lateral diffusion on SAC-modulated surface. Reproduced with permission^[101]. Copyright 2022, American Chemical Society. SAs: Single atoms; SAC: single atom catalyst.

efficiency of SACs in regulating Li plating/stripping behavior.

SUMMARY AND PERSPECTIVES

LMBs are one of the main choices for the next generation of high-energy-density batteries. However, the insufficient transport kinetics can lead to a series of problems, such as uneven deposition of Li^+ ions on the LMAs, resulting in the growth of lithium dendrites, which will reduce CE and cycling life. Secondly, the improvement of rapid charging capability also requires excellent transport ability of Li^+ ions. In practical applications, low-temperature climate environments can also increase the viscosity of the electrolyte, and decrease the ion conductivity, making it difficult for Li^+ ions to be desolvated. Therefore, it is urgent to propose effective methods to improve the transport kinetics of Li^+ ions in LMBs. In this review, we systematically summarize some of the latest strategies from four aspects: bulk electrolyte design, interfacial desolvation, tailoring the electrolyte solvation towards conductive and stronger SEI, and intrinsic design of lithium metal hosts. In recent years, remarkable achievements have been made in improving the transport kinetics of Li^+ ions. Exploring low-temperature electrolytes with a low desolvation barrier, high ionic conductivity at low temperatures, and the ability to develop inorganic-rich SEI, which could suppress dendrite growth at low temperatures, is still required. Developing advanced fast charging batteries necessitates improving Li^+ transport properties, reducing Li-plating tendency with more complex charging protocols, minimizing the ion-diffusion distance by architectural electrode design, and efficiently extracting heat from batteries as key directions of future research.

However, there is still a sufficient knowledge gap in understanding the behavior of Li^+ ion transport. The following are the key areas that we propose need to be addressed.

Quantitative and dynamic models of electrolyte solvation structure

In the past few years, the solvation structure of Li^+ ions has been extensively studied. For example, the components of the inner solvation shell of Li^+ ions will preferentially participate in the formation of the SEI and affect its stability. This view has become a consensus among electrolyte researchers. However, the current research on the solvation structure of Li^+ ions is still non-quantitative, non-dynamic, and even vague. Under the action of an electric field, the solvation structure of Li^+ ions may change, and the coordination mode and conformation of Li^+ ions with solvent molecules will also affect the transport of these ions. Therefore, it is urgently needed to introduce accurate models and precise parameters to quantify the solvation behavior of Li^+ ions.

Kinetic models, such as Kinetic Monte Carlo (KMC) simulations, are used in LMB research to investigate and forecast ion transport, dendrite development, and electrode/electrolyte interface dynamics^[102]. Future research can focus on using stand-alone KMC simulations to predict the probabilistic behavior of ions over time, capturing long-term kinetic processes and rate-limiting stages in battery events. These simulations are especially useful for investigating dendrite formation, electrodeposition, and electrolyte breakdown under a variety of circumstances.

Thorough understanding of the interfacial processes and developing advanced *in-situ* characterization

Desolvation process, charge transfer, and Li^+ ions diffusion in SEI or CEI all belong to interfacial processes; however, a precise comprehension of these processes is still lacking. For instance, it is unclear whether the ability of desolvation at interfaces is primarily determined by the strength of the binding between solvent molecules and lithium ions, or by the composition of the SEI or CEI. Moreover, what differences exist in the desolvation behavior of different Li^+ ion solvation structures? It has also been discovered that higher resistance in the desolvation process is more effective at inhibiting the Li dendrite growth (which is contrary

to most of the studies and the concept that increasing the desolvation kinetics favors rapid ion transfer and suppresses dendrites development). Therefore, it is necessary to gain a deeper understanding of the interfacial processes under the actual operating conditions of the cell. *In-situ* and operando characterization techniques can be used to observe real-time information about Li^+ ion transport modes, *etc.* In recent years, *in-situ* X-ray diffraction (XRD), Raman, X-ray absorption spectroscopy (XAS), transmission electron microscopy (TEM), sum frequency generation (SFG), and other techniques have been applied to *in situ* observations of the electrolyte-electrode interface, and more surface-sensitive techniques are still under development.

Molecular dynamics simulation and machine learning

Traditional research often relies on a trial-and-error process or accidental discoveries, which can be time-consuming and lack accurate predictions of experiments. With the development of computer technology, classical, *ab initio*, and machine learning molecular dynamics (MD) can model and compute the electrolyte-electrode interface. MD simulations play an important role in explaining the solvation structure of electrolytes, Li^+ ion transport mechanisms, and electrolyte-electrode interface reaction mechanisms. Machine learning and big data analysis can identify internal patterns of different materials, thereby providing more reliable predictions of experiments.

KMC may also be used with MD simulations to take advantage of the precise atomic-scale dynamics of MD and the long-term, larger-scale behavior anticipated by KMC. MD gives information on atomic interactions and transport parameters that may be utilized to parameterize KMC models, boosting their accuracy in forecasting battery performance and failure modes. DFT computations provide information about the electronic structure and interaction energies of materials. Integrating DFT with KMC can allow the prediction of correct energy barriers and reaction processes in KMC simulations. This combination can aid in understanding underlying processes at the atomic level and anticipating how changes in material qualities affect battery performance. Integrating these models allows researchers to get a thorough knowledge of LMB behavior, combining specific atomic-level insights with wider kinetic predictions.

Transformers, a kind of deep learning architecture, have been used to model many elements of battery dynamics, such as lithium-ion diffusion and transport kinetics. They can contribute to data-driven insights by processing and analyzing extensive datasets on battery performance, such as ion transport, diffusion rates, and cycle behavior. They aid in the identification of data patterns and linkages that might otherwise go undetected by conventional analysis. Transformers can be used to create prediction models of battery behavior under a variety of scenarios. For example, they can forecast how changes in battery materials or designs influence lithium-ion transport kinetics, which aids in battery performance improvement. Transformers can help identify new materials or improve current ones for improved lithium-ion transport by analyzing data from experiments and simulations. They can be used to discover promising electrode and electrolyte choices. Transformers can help optimize battery designs by anticipating how different design characteristics affect ion transport. This involves optimizing electrolyte compositions, electrode architectures, and overall battery configurations to increase performance.

Practical evaluation of LMBs

The evaluation of LMB performance should be more rigorous, for example, using ultrathin LMAs ($< 50 \mu\text{m}$), lean electrolytes ($< 3 \text{ g-Ah}^{-1}$), high-loading cathodes ($> 3 \text{ mAh}\cdot\text{cm}^{-2}$), high charging current density ($> 1 \text{ mA}\cdot\text{cm}^{-2}$), and extreme temperature conditions in full cell evaluation. In addition, using large-area Li pouch cells instead of coin cells to evaluate battery performance is more in line with the needs of large-scale production and practical applications. The calculation of the actual energy density of the battery should include all materials in a reasonable data unit, such as the mass of the separator, electrolyte, and sealing film.

DECLARATIONS

Authors' contributions

Wrote original manuscript draft: Mushtaq, F.; Tu, H.; Liu, M.

Made substantial contributions to conception and design of the study and revised the manuscript: Mushtaq, F.; Tu, H.; Zheng, Y.; Wang, Z.; Hou, M.

Provided administrative, technical, and material support: Zhang, Y.; Liu, M.; Liu, J.; Chen, K.; Liang, F.; Liu, F.; Zou, B.; Xue, D.

Availability of data and materials

Not applicable.

Financial support and sponsorship

This work was supported by the National Natural Science Foundation of China (22075313, 22379160, 52220105010), Guangdong Basic and Applied Basic Research Foundation (2022A1515140165), Outstanding Youth Fund of Jiangxi Province (20192BCB23028), and Jiangxi Double Thousand Talent Program (JXSQ2019101072), Mushtaq F kindly acknowledges the financial support of ANSO Scholarship for Young Talents.

Conflicts of interest

All authors declared that there are no conflicts of interest.

Ethical approval and consent

Not applicable.

Consent for publication

Not applicable.

Copyright

© The Author(s) 2025.

REFERENCES

1. Gupta, A.; Manthiram, A. Designing advanced lithium-based batteries for low-temperature conditions. *Adv. Energy. Mater.* **2020**, *10*, 2001972. DOI PubMed PMC
2. Li, L.; Wang, M.; Wang, J.; et al. Asymmetric gel polymer electrolyte with high lithium ion conductivity for dendrite-free lithium metal batteries. *J. Mater. Chem. A*. **2020**, *8*, 8033-40. DOI
3. Hu, A.; Li, F.; Chen, W.; et al. Ion transport kinetics in low-temperature lithium metal batteries. *Adv. Energy. Mater.* **2022**, *12*, 2202432. DOI
4. Hao, Z.; Wu, Y.; Zhao, Q.; et al. Functional separators regulating ion transport enabled by metal-organic frameworks for dendrite-free lithium metal anodes. *Adv. Funct. Mater.* **2021**, *31*, 2102938. DOI
5. Tu, H.; Li, L.; Wang, Z.; et al. Tailoring electrolyte solvation for LiF-rich solid electrolyte interphase toward a stable Li anode. *ACS. Nano*. **2022**, *16*, 16898-908. DOI PubMed
6. Hwang, G.; Sitapure, N.; Moon, J.; Lee, H.; Hwang, S.; Sang-il, K. J. Model predictive control of lithium-ion batteries: development of optimal charging profile for reduced intracycle capacity fade using an enhanced single particle model (SPM) with first-principled chemical/mechanical degradation mechanisms. *Chem. Eng. J.* **2022**, *435*, 134768. DOI
7. Sarkar, S.; Zohra, H. S.; El-halwagi, M. M.; Khan, F. I. Electrochemical models: methods and applications for safer lithium-ion battery operation. *J. Electrochem. Soc.* **2022**, *169*, 100501. DOI
8. Pang, H.; Wu, L.; Liu, J.; Liu, X.; Liu, K. Physics-informed neural network approach for heat generation rate estimation of lithium-ion battery under various driving conditions. *J. Energy. Chem.* **2023**, *78*, 1-12. DOI
9. Cao, T.; Huang, S.; Sun, Y.; et al. Fluorine-rich interphase and desolvation regulation for a long-life and high-rate TiS₂-based Li-metal battery. *J. Phys. Chem. C*. **2022**, *126*, 5122-30. DOI

10. Wang, Z.; Qi, F.; Yin, L.; et al. An anion-tuned solid electrolyte interphase with fast ion transfer kinetics for stable lithium anodes. *Adv. Energy. Mater.* **2020**, *10*, 1903843. DOI
11. Wang, Y.; Tu, H.; Sun, A.; et al. Dual Li^+ transport enabled by BN-assisted solid-polymer-electrolyte for high-performance lithium batteries. *Chem. Eng. J.* **2023**, *475*, 146414. DOI
12. Wang, L.; Yi, S.; Liu, Q.; et al. Bifunctional lithium-montmorillonite enabling solid electrolyte with superhigh ionic conductivity for high-performanced lithium metal batteries. *Energy. Storage. Mater.* **2023**, *63*, 102961. DOI
13. Zhang, J.; He, R.; Zhuang, Q.; et al. Tuning 4f-center electron structure by Schottky defects for catalyzing Li diffusion to achieve long-term dendrite-free lithium metal battery. *Adv. Sci.* **2022**, *9*, e2202244. DOI PubMed PMC
14. Chen, J.; Li, Z.; Sun, N.; et al. A robust Li-intercalated interlayer with strong electron withdrawing ability enables durable and high-rate Li metal anode. *ACS. Energy. Lett.* **2022**, *7*, 1594-603. DOI
15. Zhang, N.; Deng, T.; Zhang, S.; et al. Critical review on low-temperature Li-ion/metal batteries. *Adv. Mater.* **2022**, *34*, e2107899. DOI PubMed
16. Xu, J.; Zhang, J.; Pollard, T. P.; et al. Electrolyte design for Li-ion batteries under extreme operating conditions. *Nature* **2023**, *614*, 694-700. DOI PubMed
17. Feng, Y.; Zhou, L.; Ma, H.; et al. Challenges and advances in wide-temperature rechargeable lithium batteries. *Energy. Environ. Sci.* **2022**, *15*, 1711-59. DOI
18. Suo, L.; Borodin, O.; Gao, T.; et al. "Water-in-salt" electrolyte enables high-voltage aqueous lithium-ion chemistries. *Science* **2015**, *350*, 938-43. DOI PubMed
19. Suo, L.; Hu, Y. S.; Li, H.; Armand, M.; Chen, L. A new class of solvent-in-salt electrolyte for high-energy rechargeable metallic lithium batteries. *Nat. Commun.* **2013**, *4*, 1481. DOI PubMed
20. Chen, S.; Zheng, J.; Mei, D.; et al. High-voltage lithium-metal batteries enabled by localized high-concentration electrolytes. *Adv. Mater.* **2018**, *30*, e1706102. DOI PubMed
21. Chu, F.; Deng, R.; Wu, F. Unveiling the effect and correlative mechanism of series-dilute electrolytes on lithium metal anodes. *Energy. Storage. Mater.* **2023**, *56*, 141-54. DOI
22. Sun, N.; Li, R.; Zhao, Y.; et al. Anionic coordination manipulation of multilayer solvation structure electrolyte for high-rate and low-temperature lithium metal battery. *Adv. Energy. Mater.* **2022**, *12*, 2200621. DOI
23. Ma, T.; Ni, Y.; Wang, Q.; et al. Optimize lithium deposition at low temperature by weakly solvating power solvent. *Angew. Chem. Int. Ed. Engl.* **2022**, *61*, e202207927. DOI PubMed
24. Tian, C.; Qin, K.; Suo, L. Concentrated electrolytes for rechargeable lithium metal batteries. *Mater. Futures.* **2023**, *2*, 012101. DOI
25. Yu, Z.; Balsara, N. P.; Borodin, O.; et al. Beyond local solvation structure: nanometric aggregates in battery electrolytes and their effect on electrolyte properties. *ACS. Energy. Lett.* **2022**, *7*, 461-70. DOI
26. Liu, W.; Yi, C.; Li, L.; et al. Designing polymer-in-salt electrolyte and fully infiltrated 3D electrode for integrated solid-state lithium batteries. *Angew. Chem. Int. Ed. Engl.* **2021**, *60*, 12931-40. DOI PubMed
27. Hu, Y.; Li, L.; Tu, H.; et al. Janus electrolyte with modified Li^+ solvation for high-performance solid-state lithium batteries. *Adv. Funct. Mater.* **2022**, *32*, 2203336. DOI
28. Du, L.; Zhang, B.; Yang, C.; Cui, L.; Mai, L.; Xu, L. Leaf-inspired quasi-solid electrolyte enables uniform lithium deposition and suppressed lithium-electrolyte reactions for lithium metal batteries. *Energy. Storage. Mater.* **2023**, *61*, 102914. DOI
29. Zheng, G.; Yan, T.; Hong, Y.; et al. A non-Newtonian fluid quasi-solid electrolyte designed for long life and high safety Li-O₂ batteries. *Nat. Commun.* **2023**, *14*, 2268. DOI PubMed PMC
30. Zeng, X.; Yin, Y.; Shi, Y.; et al. Lithiation-derived repellent toward lithium anode safeguard in quasi-solid batteries. *Chem* **2018**, *4*, 298-307. DOI
31. Kim, M. S.; Zhang, Z.; Rudnicki, P. E.; et al. Suspension electrolyte with modified Li^+ solvation environment for lithium metal batteries. *Nat. Mater.* **2022**, *21*, 445-54. DOI PubMed
32. Kim, M. S.; Zhang, Z.; Wang, J.; et al. Revealing the multifunctions of Li_3N in the suspension electrolyte for lithium metal batteries. *ACS. Nano.* **2023**, *17*, 3168-80. DOI PubMed
33. Tu, H.; He, Z.; Sun, A.; et al. Superior Li^+ kinetics by "Low-Activity-Solvent" engineering for stable lithium metal batteries. *Nano. Lett.* **2024**, *24*, 5714-21. DOI PubMed
34. Huang, X.; Li, R.; Sun, C.; et al. Solvent-assisted hopping mechanism enables ultrafast charging of lithium-ion batteries. *ACS. Energy. Lett.* **2022**, *7*, 3947-57. DOI
35. Sun, C.; Ji, X.; Weng, S.; et al. 50C fast-charge Li-ion batteries using a graphite anode. *Adv. Mater.* **2022**, *34*, e2206020. DOI PubMed
36. Chen, Y.; Yu, Z.; Rudnicki, P.; et al. Steric effect tuned ion solvation enabling stable cycling of high-voltage lithium metal battery. *J. Am. Chem. Soc.* **2021**, *143*, 18703-13. DOI PubMed
37. Park, E.; Park, J.; Lee, K.; et al. Exploiting the steric effect and low dielectric constant of 1,2-dimethoxypropane for 4.3 V lithium metal batteries. *ACS. Energy. Lett.* **2023**, *8*, 179-88. DOI
38. Yao, Y. X.; Chen, X.; Yan, C.; et al. Regulating interfacial chemistry in lithium-ion batteries by a weakly solvating electrolyte. *Angew. Chem. Int. Ed. Engl.* **2021**, *60*, 4090-7. DOI PubMed
39. Li, Z.; Rao, H.; Atwi, R.; et al. Non-polar ether-based electrolyte solutions for stable high-voltage non-aqueous lithium metal batteries. *Nat. Commun.* **2023**, *14*, 868. DOI PubMed PMC

40. Yu, Z.; Rudnicki, P. E.; Zhang, Z.; et al. Rational solvent molecule tuning for high-performance lithium metal battery electrolytes. *Nat. Energy*. **2022**, *7*, 94-106. DOI
41. Wang, H.; Yu, Z.; Kong, X.; et al. Dual-solvent Li-ion solvation enables high-performance Li-metal batteries. *Adv. Mater.* **2021**, *33*, e2008619. DOI PubMed
42. Tan, L.; Chen, S.; Chen, Y.; et al. Intrinsic nonflammable ether electrolytes for ultrahigh-voltage lithium metal batteries enabled by chlorine functionality. *Angew. Chem. Int. Ed. Engl.* **2022**, *61*, e202203693. DOI PubMed
43. Ruan, D.; Tan, L.; Chen, S.; et al. Solvent versus anion chemistry: unveiling the structure-dependent reactivity in tailoring electrochemical interphases for lithium-metal batteries. *JACS. Au*. **2023**, *3*, 953-63. DOI PubMed PMC
44. Shi, J.; Xu, C.; Lai, J.; et al. An amphiphilic molecule-regulated core-shell-solvation electrolyte for Li-metal batteries at ultra-low temperature. *Angew. Chem. Int. Ed. Engl.* **2023**, *62*, e202218151. DOI PubMed
45. Zhao, Y.; Zhou, T.; Ashirov, T.; et al. Fluorinated ether electrolyte with controlled solvation structure for high voltage lithium metal batteries. *Nat. Commun.* **2022**, *13*, 2575. DOI PubMed PMC
46. Dou, Q.; Yao, N.; Pang, W. K.; et al. Unveiling solvation structure and desolvation dynamics of hybrid electrolytes for ultralong cyclability and facile kinetics of Zn–Al alloy anodes. *Energy. Environ. Sci.* **2022**, *15*, 4572-83. DOI
47. Tanibata, N.; Morimoto, R.; Nishikawa, K.; Takeda, H.; Nakayama, M. Asymmetry in the solvation-desolvation resistance for Li metal batteries. *Anal. Chem.* **2020**, *92*, 3499-502. DOI PubMed
48. Feng, Y.; Zhong, B.; Zhang, R.; et al. Achieving high-power and dendrite-free lithium metal anodes via interfacial ion-transport-rectifying pump. *Adv. Energy. Mater.* **2023**, *13*, 2203912. DOI
49. Yao, S.; Yang, Y.; Liang, Z.; et al. A dual-functional cationic covalent organic frameworks modified separator for high energy lithium metal batteries. *Adv. Funct. Mater.* **2023**, *33*, 2212466. DOI
50. Bai, S.; Sun, Y.; Yi, J.; He, Y.; Qiao, Y.; Zhou, H. High-power Li-metal anode enabled by metal-organic framework modified electrolyte. *Joule* **2018**, *2*, 2117-32. DOI
51. Chang, Z.; Qiao, Y.; Yang, H.; et al. Beyond the concentrated electrolyte: further depleting solvent molecules within a Li⁺ solvation sheath to stabilize high-energy-density lithium metal batteries. *Energy. Environ. Sci.* **2020**, *13*, 4122-31. DOI
52. Jiang, C.; Gu, Y.; Tang, M.; et al. Toward stable lithium plating/stripping by successive desolvation and exclusive transport of Li ions. *ACS. Appl. Mater. Interfaces*. **2020**, *12*, 10461-70. DOI PubMed
53. Li, L.; Tu, H.; Wang, J.; et al. Electrocatalytic MOF-carbon bridged network accelerates Li⁺-solvents desolvation for high Li⁺ diffusion toward rapid sulfur redox kinetics. *Adv. Funct. Mater.* **2023**, *33*, 2212499. DOI
54. Xu, Y.; Gao, L.; Shen, L.; et al. Ion-transport-rectifying layer enables Li-metal batteries with high energy density. *Matter* **2020**, *3*, 1685-700. DOI
55. Chang, Z.; Qiao, Y.; Deng, H.; Yang, H.; He, P.; Zhou, H. A liquid electrolyte with de-solvated lithium ions for lithium-metal battery. *Joule* **2020**, *4*, 1776-89. DOI
56. Li, C.; Lu, R.; Amin, K.; et al. Robust anion-shielding metal-organic frameworks based composite interlayers to achieve uniform Li deposition for stable Li-metal anode. *ChemElectroChem* **2022**, *9*, e202101596. DOI
57. Yang, Y.; Yao, S.; Liang, Z.; et al. A self-supporting covalent organic framework separator with desolvation effect for high energy density lithium metal batteries. *ACS. Energy. Lett.* **2022**, *7*, 885-96. DOI
58. Wang, X.; Wang, H.; Liu, M.; Li, W. In-plane lithium growth enabled by artificial nitrate-rich layer: fast deposition kinetics and desolvation/adsorption mechanism. *Small* **2020**, *16*, e2000769. DOI PubMed
59. Wang, J.; Hu, H.; Duan, S.; et al. Construction of moisture-stable lithium diffusion-controlling layer toward high performance dendrite-free lithium anode. *Adv. Funct. Mater.* **2022**, *32*, 2110468. DOI
60. Zhang, W.; Shen, Z.; Li, S.; et al. Engineering wavy-nanostructured anode interphases with fast ion transfer kinetics: toward practical Li-metal full batteries. *Adv. Funct. Mater.* **2020**, *30*, 2003800. DOI
61. Wang, J.; Zhang, J.; Wu, J.; et al. Interfacial “Single-atom-in-defects” catalysts accelerating Li⁺ desolvation kinetics for long-lifespan lithium-metal batteries. *Adv. Mater.* **2023**, *35*, e2302828. DOI PubMed
62. Wang, J.; Zhang, J.; Cheng, S.; et al. Long-life dendrite-free lithium metal electrode achieved by constructing a single metal atom anchored in a diffusion modulator layer. *Nano. Lett.* **2021**, *21*, 3245-53. DOI
63. Wen, P.; Liu, Y.; Mao, J.; et al. Tuning desolvation kinetics of in-situ weakly solvating polyacetal electrolytes for dendrite-free lithium metal batteries. *J. Energy. Chem.* **2023**, *79*, 340-7. DOI
64. Xu, K. Interfaces and interphases in batteries. *J. Power. Sources*. **2023**, *559*, 232652. DOI
65. Tu, H.; Li, L.; Hu, Y.; et al. Non-flammable liquid polymer-in-salt electrolyte enabling secure and dendrite-free lithium metal battery. *Chem. Eng. J.* **2022**, *434*, 134647. DOI
66. Fong, R.; von, S. U.; Dahn, J. R. Studies of lithium intercalation into carbons using nonaqueous electrochemical cells. *J. Electrochem. Soc.* **1990**, *137*, 2009-13. DOI
67. Wang, L.; Menakath, A.; Han, F.; et al. Identifying the components of the solid-electrolyte interphase in Li-ion batteries. *Nat. Chem.* **2019**, *11*, 789-96. DOI
68. Hu, Z.; Zhang, S.; Dong, S.; Li, Q.; Cui, G.; Chen, L. Self-stabilized solid electrolyte interface on a host-free Li-metal anode toward high areal capacity and rate utilization. *Chem. Mater.* **2018**, *30*, 4039-47. DOI
69. Wang, Z.; Zhang, F.; Sun, Y.; et al. Intrinsically nonflammable ionic liquid-based localized highly concentrated electrolytes enable high-performance Li-metal batteries. *Adv. Energy. Mater.* **2021**, *11*, 2003752. DOI

70. Xie, J.; Sun, S. Y.; Chen, X.; et al. Fluorinating the solid electrolyte interphase by rational molecular design for practical lithium-metal batteries. *Angew. Chem. Int. Ed. Engl.* **2022**, *61*, e202204776. DOI PubMed
71. Zhu, C.; Sun, C.; Li, R.; et al. Anion–diluent pairing for stable high-energy Li metal batteries. *ACS. Energy. Lett.* **2022**, *7*, 1338–47. DOI
72. Sun, A.; Tu, H.; Sun, Z.; et al. Dual-halide interphase enabling high-performance lithium metal batteries in wide-temperature range. *ACS. Energy. Lett.* **2024**, *9*, 2545–53. DOI
73. Zhang, S.; Li, R.; Hu, N.; et al. Tackling realistic Li^+ flux for high-energy lithium metal batteries. *Nat. Commun.* **2022**, *13*, 5431. DOI PubMed PMC
74. Liu, S.; Ji, X.; Piao, N.; et al. An inorganic-rich solid electrolyte interphase for advanced lithium-metal batteries in carbonate electrolytes. *Angew. Chem. Int. Ed. Engl.* **2021**, *60*, 3661–71. DOI PubMed
75. Zhang, W.; Wu, Q.; Huang, J.; et al. Colossal granular lithium deposits enabled by the grain-coarsening effect for high-efficiency lithium metal full batteries. *Adv. Mater.* **2020**, *32*, e2001740. DOI PubMed
76. Yan, C.; Li, H. R.; Chen, X.; et al. Regulating the inner Helmholtz plane for stable solid electrolyte interphase on lithium metal anodes. *J. Am. Chem. Soc.* **2019**, *141*, 9422–9. DOI PubMed
77. Wang, Q.; Yao, Z.; Zhao, C.; et al. Interface chemistry of an amide electrolyte for highly reversible lithium metal batteries. *Nat. Commun.* **2020**, *11*, 4188. DOI PubMed PMC
78. Wu, D.; He, J.; Liu, J.; et al. $\text{Li}_2\text{CO}_3/\text{LiF}$ -rich heterostructured solid electrolyte interphase with superior lithiophilic and Li^+ -transferred characteristics via adjusting electrolyte additives. *Adv. Energy. Mater.* **2022**, *12*, 2200337. DOI
79. Mao, M.; Ji, X.; Wang, Q.; et al. Anion-enrichment interface enables high-voltage anode-free lithium metal batteries. *Nat. Commun.* **2023**, *14*, 1082. DOI PubMed PMC
80. Zeng, H.; Yu, K.; Li, J.; et al. Beyond LiF : tailoring Li_2O -dominated solid electrolyte interphase for stable lithium metal batteries. *ACS. Nano.* **2024**, *18*, 1969–81. DOI PubMed
81. Wang, J.; Yang, J.; Xiao, Q.; et al. In situ self-assembly of ordered organic/inorganic dual-layered interphase for achieving long-life dendrite-free Li metal anodes in LiFSI-based electrolyte. *Adv. Funct. Mater.* **2021**, *31*, 2007434. DOI
82. Wang, Z.; Zhang, H.; Xu, J.; et al. Advanced ultralow-concentration electrolyte for wide-temperature and high-voltage Li-metal batteries. *Adv. Funct. Mater.* **2022**, *32*, 2112598. DOI
83. Yan, C.; Cheng, X. B.; Tian, Y.; et al. Dual-layered film protected lithium metal anode to enable dendrite-free lithium deposition. *Adv. Mater.* **2018**, *30*, e1707629. DOI PubMed
84. Li, Z.; Yu, R.; Weng, S.; Zhang, Q.; Wang, X.; Guo, X. Tailoring polymer electrolyte ionic conductivity for production of low-temperature operating quasi-all-solid-state lithium metal batteries. *Nat. Commun.* **2023**, *14*, 482. DOI PubMed PMC
85. Lin, H.; Zhang, Z.; Wang, Y.; Zhang, X. L.; Tie, Z.; Jin, Z. Template-sacrificed hot fusion construction and nanoseed modification of 3D porous copper nanoscaffold host for stable-cycling lithium metal anodes. *Adv. Funct. Mater.* **2021**, *31*, 2102735. DOI
86. Guan, W.; Hu, X.; Liu, Y.; et al. Advances in the emerging gradient designs of Li metal hosts. *Research* **2022**, *2022*, 9846537. DOI PubMed PMC
87. Bai, M.; Xie, K.; Yuan, K.; et al. A scalable approach to dendrite-free lithium anodes via spontaneous reduction of spray-coated graphene oxide layers. *Adv. Mater.* **2018**, *30*, e1801213. DOI PubMed
88. Li, Q.; Zhu, S.; Lu, Y. 3D porous Cu current collector/Li-metal composite anode for stable lithium-metal batteries. *Adv. Funct. Mater.* **2017**, *27*, 1606422. DOI
89. Wang, J.; Li, L.; Hu, H.; et al. Toward dendrite-free metallic lithium anodes: from structural design to optimal electrochemical diffusion kinetics. *ACS. Nano.* **2022**, *16*, 17729–60. DOI PubMed
90. Yi, J.; Chen, J.; Yang, Z.; et al. Facile Patterning of laser-induced graphene with tailored Li nucleation kinetics for stable lithium-metal batteries. *Adv. Energy. Mater.* **2019**, *9*, 1901796. DOI
91. Shen, X.; Zhao, G.; Yu, X.; Huang, H.; Wang, M.; Zhang, N. Multifunctional SnSe-C composite modified 3D scaffolds to regulate lithium nucleation and fast transport for dendrite-free lithium metal anodes. *J. Mater. Chem. A.* **2021**, *9*, 21695–702. DOI
92. Wang, X.; Pan, Z.; Wu, Y.; et al. Reducing lithium deposition overpotential with silver nanocrystals anchored on graphene aerogel. *Nanoscale* **2018**, *10*, 16562–7. DOI PubMed
93. Gu, Y.; Li, C.; Wang, Y.; Lu, W.; Shang, H.; Sun, B. Precise construction of lithiophilic sites by diyne-linked phthalocyanine polymer for suppressing metallic lithium dendrite. *Dalton. Trans.* **2022**, *51*, 5828–33. DOI PubMed
94. Duan, H.; Zhang, J.; Chen, X.; et al. Uniform nucleation of lithium in 3D current collectors via bromide intermediates for stable cycling lithium metal batteries. *J. Am. Chem. Soc.* **2018**, *140*, 18051–7. DOI PubMed
95. Huang, K.; Li, Z.; Xu, Q.; Liu, H.; Li, H.; Wang, Y. Lithiophilic CuO nanoflowers on Ti-mesh inducing lithium lateral plating enabling stable lithium-metal anodes with ultrahigh rates and ultralong cycle life. *Adv. Energy. Mater.* **2019**, *9*, 1900853. DOI
96. Chen, X.; Li, B.; Zhao, C.; Zhang, R.; Zhang, Q. Synergetic coupling of lithiophilic sites and conductive scaffolds for dendrite-free lithium metal anodes. *Small. Methods.* **2020**, *4*, 1900177. DOI
97. Shen, X.; Shi, S.; Li, B.; et al. Lithiophilic interphase porous buffer layer toward uniform nucleation in lithium metal anodes. *Adv. Funct. Mater.* **2022**, *32*, 2206388. DOI
98. Gu, J.; Zhu, Q.; Shi, Y.; et al. Single zinc atoms immobilized on MXene ($\text{Ti}_3\text{C}_2\text{Cl}_x$) layers toward dendrite-free lithium metal anodes. *ACS. Nano.* **2020**, *14*, 891–8. DOI PubMed
99. Xu, K.; Zhu, M.; Wu, X.; et al. Dendrite-tamed deposition kinetics using single-atom Zn sites for Li metal anode. *Energy. Storage.*

- Mater.* **2019**, *23*, 587-93. DOI
100. Yang, Z.; Dang, Y.; Zhai, P.; et al. Single-atom reversible lithiophilic sites toward stable lithium anodes. *Adv. Energy. Mater.* **2022**, *12*, 2103368. DOI
101. Wang, J.; Zhang, J.; Duan, S.; et al. Lithium atom surface diffusion and delocalized deposition propelled by atomic metal catalyst toward ultrahigh-capacity dendrite-free lithium anode. *Nano. Lett.* **2022**, *22*, 8008-17. DOI PubMed
102. Lee, H.; Sitapure, N.; Hwang, S.; Kwon, J. S. Multiscale modeling of dendrite formation in lithium-ion batteries. *Comput. Chem. Eng.* **2021**, *153*, 107415. DOI



Farwa Mushtaq

Farwa Mushtaq received her master's degree in chemistry from the University of Agriculture Faisalabad, Pakistan, in 2018. She is currently a Ph.D. candidate at the School of Nanotech and Nanobionics, University of Science and Technology of China, Chinese Academy of Sciences. Her research focuses on lithium metal batteries and electrolytes.



Haifeng Tu

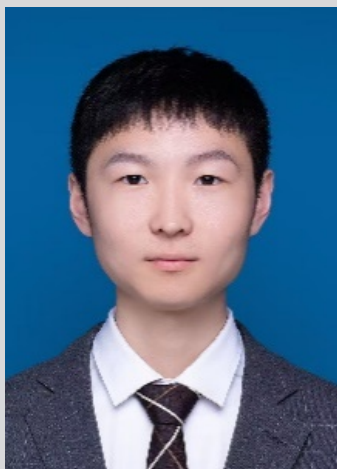
Haifeng Tu is a Ph.D. student at the University of Science and Technology of China, with a research focus on the design of electrolytes for high-energy lithium metal batteries and the study of interface chemistry. His current work centers on the synthesis and development of ionic liquid-based electrolytes. To date, he has published 9 papers as the first/co-first author in journals such as *Angew. Chem.*, *Nano Lett.*, *ACS Energy Lett.*, *ACS nano*, *AFM*, etc.

**Yuting Zheng**

Yuting Zheng obtained his bachelor's degree from Tiangong University in 2021. He is currently a postgraduate at the University of Science and Technology of China. His current scientific interest focuses on solid-state electrolytes for lithium metal batteries.

**Yongyi Zhang**

Yongyi Zhang received his Ph.D. from Peking University in 2008 and then conducted postdoctoral research at the University of Michigan and University of South Dakota, USA. He is currently a Professor at the Suzhou Institute of Nanotechnology, CAS, and the director of the Department of Nanomaterials at Jiangxi Institute of Nanotechnology. He has mainly engaged in the continuous preparation and innovative application research of olefinic carbon fibers and high-performance technology of carbon nanotube fibers.

**Zhiqiang Wang**

Zhiqiang Wang is a doctoral student in Materials and Chemical Engineering at Shandong University. His research primarily focuses on the preparation of electrochemical energy storage materials and the growth of large-size lithium niobate crystals.

**Minjie Hou**

Minjie Hou is a lecturer at Kunming University of Science and Technology. His research focuses on solid-state sodium-ion batteries, plasma-modified energy materials and their applications in electrochemical energy storage and conversion.

**Meinan Liu**

Dr. Meinan Liu is currently a professor in Guangxi University. She received her Ph.D. in Chemical Technology from Dalian University of Technology in 2009. After completing her Ph.D., she conducted research at Queensland University of Technology and Suzhou Institute of Nanotechnology and Nano-bionics, Chinese Academy of Sciences. Her current research interests include the synthesis, characterization, and applications of nanomaterials in energy conversion/storage.

**Kunfeng Chen**

Dr. Kunfeng Chen is a full professor at Shandong University. He is mainly engaged in the research of electrochemical energy storage materials, single crystal growth, and optoelectronic devices. He has published over 100 research papers and has an H-index of 43.

**Feng Liang**

Dr. Feng Liang is a full professor in Kunming University of Science and Technology and a visiting professor of Kyushu University in Japan. He received his Ph.D. in Environmental Chemistry from the Tokyo Institute of Technology, Japan, in 2014. His research focuses on metal-air/CO₂ batteries, solid-state batteries, plasma preparation and modification nanomaterials, and their application for electrochemical energy storage and conversion.

**Jun Liu**

Dr. Jun Liu is a professor of Materials Science and Engineering at South China University of Technology, China. He received his Ph.D. in chemical engineering from Dalian University of Technology in 2010. From 2012 to 2015, he worked as a postdoctoral researcher at Deakin University and Max Planck Institute for Solid State Research. His current research interests mainly include the design of novel electrodes and electrolytes for rechargeable batteries, especially for Li-/Na-ion and all-solid-state batteries.

**Fei Liu**

Dr. Fei Liu received his Bachelor's and Ph.D. degrees from Dalian University of Technology under the supervision of Professor Dongfeng Xue. He then worked as a postdoctoral researcher in the Korea Research Institute of Chemical Technology for one year before joining the University of Manchester, UK, as a research associate. His current research interests focus on the design of electrode materials for energy storage.

**Bingsuo Zou**

Dr. Bingsuo Zou received his B.S. degree from Jilin University in 1985 and his Ph.D. from Jilin University in 1991. He worked as an associate Research Scientist at the Institute of Physics, Chinese Academy of Sciences, starting in 1994. In 2000, he was selected as one of the hundred talents of CAS. In 2005, he moved to Hunan University as a Professor at the School of Physics. In 2009, He moved to the Beijing Institute of Technology as the dean and professor of the School of Materials. In 2019, he moved to Guangxi University as a Professor. His research focuses on optoelectronic materials, nanophotonics, and optics of magnetic semiconductors.

**Dongfeng Xue**

Dr. Dongfeng Xue is a full professor at the Shenzhen Institute for Advanced Study, University of Electronic Science and Technology of China. His research interests focus on crystal growth theory, large-size crystal growth technology, and multiscale materials design for boosting their functionalities. He has co-authored more than 700 journal articles and has an H-index of 71. He is a Fellow of the Royal Society of Chemistry and serves as an associate editor for *CrystEngComm* and on the editorial boards of *Journal of Crystal Growth*, *Science China-Technological Sciences*, *Journal of Rare Earths*, etc.